Serological and spatio-temporal analysis of anthrax in Mongolia

(モンゴルにおける炭疽の血清学的解析と時空間分析)

Tuvshinzaya Zorigt

Division of Infection and Immunity

International Institute for Zoonosis Control

Graduate School of Infectious Diseases

Hokkaido University

2022

Contents

Abbreviations

AMP	Adenosine monophosphate
Bcbva	*Bacillus cereus* biovar anthracis
CBB	Coomassie brilliant blue
CapA	Capsule biosynthesis protein CapA
CapA322	C-terminal region of CapA
cAMP	Cyclic adenosine monophosphate
CDS	coding sequence
SCVL	State Central Veterinary Laboratory
DTT	Dithiothreitol
EDTA	Ethylenediaminetetraacetic acid
EF	Edema factor
ELISA	Enzyme-linked immunosorbent assay
GST	Glutathione S transferase
GIS	Geographic information system
HiConEnv	Upper confidence envelope
IgG	Immunoglobulin G
IPTG	Isopropyl β-D-thiogalactopyranoside
KDE	Kernel density estimation
KPL	3,3′,5,5′-tetramethylbenzidine substrate
LB	Lysogeny broth
LF	Lethal factor
LoConEnv	Lower confidence envelope
MES	2-(N-morpholino) ethane sulfonic acid
Mw	Molecular weight
NaCl	Sodium chloride
NC	Negative control
NLPC/60	papain-like cell wall hydrolase domain
NLRP1	NLR family, pyrin domain containing 1
OD	Optical density
OIE	World Organization for Animal Health

PA	Protective antigen
PBS	Phosphate buffer saline
PC	Positive control
PCR	Polymerase chain reaction
PMSF	Phenylmethylsulphonyl fluoride
PMB	Polychrome methylene blue
PAD1	Recombinant protective antigen domain 1
PAGE	Polyacrylamide gel electrophoresis
rpm	Rotations per minute
RT	Room temperature
SDE	Standard deviational ellipse
SDS	Sodium dodecyl sulfate
SDS-PAGE	SDS polyacrylamide gel electrophoresis
TMB	3,3',5,5' tetramethylbenzidine
TMHMM	transmembrane-hidden Markov model
TB	Terrific broth
Vac_H	Vaccinated horse serum
WB	Western blotting
WHO	World Health Organization
γ-D-PGA	poly-γ-D-glutamic acid

78

Unit abbreviations

%	percent
g	gram
kDa	kilodalton
km^2	square kilometer
km	kilometer
L	liter
max	maximum
min	minimum
ml	milliliters
mM	millimolar
ng	nanogram
µg	microgram
µl	microliter
ºC	degree Celsius

Notes

The contents of Chapter I and Chapter II have been published in *PLoS One*.

Tuvshinzaya Zorigt, Yoshikazu Furuta, Manyando Simbotwe, Akihiro Ochi, Mai Tsujinouchi, Misheck Shawa, Tomoko Shimizu, Norikazu Isoda, Jargalsaikhan Enkhtuya, and Hideaki Higashi. **Development of ELISA based on *Bacillus anthracis* capsule biosynthesis protein CapA for naturally acquired antibodies against anthrax**. *PLoS One*. 2021; 16(10):e0258317.

Tuvshinzaya Zorigt, Satoshi Ito, Norikazu Isoda, Yoshikazu Furuta, Misheck Shawa, Natsagdorj Norov, Baasansuren Lkham, Jargalsaikhan Enkhtuya, Hideaki Higashi. **Risk factors and spatio-temporal patterns of livestock anthrax in Khuvsgul Province, Mongolia**. *PLoS One*. 2021; 16(11):e0260299.

Preface

Humans have a long history with anthrax, and outbreaks were recorded in the Bible as the sixth plague in Egypt around 5000 BC (Ben-Noun, 2002). German microbiologist Robert Koch first cultured the causative agent *Bacillus anthracis* in 1876; since then, anthrax has been studied for some 140 years (Koch, 1876). Regardless of this, pathogenesis, ecology, and epidemiology of the disease in animals remain surprisingly poorly understood.

Anthrax causative agent, *B. anthracis*, is a Gram-positive, spore-forming, non-motile, rod-shaped bacterium (Mock and Fouet, 2001). *B. anthracis* has two different lifestyles, the vegetative bacilli and a dormant spore. Anthrax is not directly transmissible between animals; instead, herbivores such as cattle and horses are infected primarily via ingesting a high dose of spores from grazing pastures. Within the host, *B. anthracis* spores germinate and form vegetative bacteria capable of multiplying and producing virulence factors, which lead to potentially fatal disease (Hugh-Jones and de Vos, 2002). When the infection is fatal to the host, vegetative cells of *B. anthracis* are shed into the soil, forming infectious spores capable of long-term survival. Furthermore, the places where an animal dies and/or their carcass disposal sites most often serve as the source of future infection (Beyer and Turnbull, 2009). In addition, spores are highly resistant to environmental stress, such as UV light, heat, and chemical disinfectants (Stephens, 1998).

Cattle exhibit dose-dependent clinical symptoms against orally given *B. anthracis* spores (Schlingman et al., 1956). Oral administration of 10^9 spores culminates in peracute death in cattle, but lower doses cause either subclinical or inapparent infections. In comparison, carnivores and birds are pretty resistant and often have naturally acquired antibodies to anthrax. These antibodies are less common in herbivores, which may have led to the assumption that anthrax is always fatal to these animals (Hugh-Jones and de Vos, 2002). However, susceptibility to anthrax varies widely among species because of inherited genetic factors, immunological state, coinfection, and physiological condition. Even within a susceptible species, there is considerable evidence that individuals survive exposure to anthrax (Turnbull et al., 1992).

Inhaling the spores, handling and slaughtering infected livestock, or consuming contaminated meat and meat products can lead to pulmonary, cutaneous, and gastrointestinal anthrax disease in humans (Kaufmann and Dannenberg, 2002). In addition, an unusual route of infection via intravenous injection of heroin contaminated with *B. anthracis* spores has been reported to be associated with several deaths in England, Scotland, and Germany (Price et al., 2012).

Anthrax is distributed across the globe, from the tropics to frigid polar regions. Outbreaks behave very differently worldwide, and the seasonality, frequency, and dynamics of anthrax are poorly understood. After an animal vaccine invention, anthrax has been drastically decreased in many parts of the world, and anthrax has become a minor concern of veterinary and public health. However, the adverse consequence was a loss of interest and increasing failure to diagnose and stop animal mass vaccination. Today, anthrax is still regarded as endemic among the livestock in Africa, Asia, and several countries of the former Soviet Union and tends to re-emerge in countries due to climate changes (Fasanella et al., 2010). The re-emergence of anthrax in Siberia showed how an increase in summer air temperature triggered the outbreak through the effect of permafrost thawing, which might release the spores from formerly infected carcasses (Liskova et al., 2021). This phenomenon entails that the process of permafrost degradation and thawing rates of its active layer potentially lead to the re-emergence of pathogens, particularly anthrax in the northern latitude of the globe, where the warming effect is more pronounced. Hence, there are interdisciplinary research is necessary to understand this disease.

Anthrax is hyperendemic in the northern region and endemic in areas of Mongolia except the desert region in the south (Odontsetseg et al., 2007). Frequent outbreaks occur in wildlife and livestock, taking their toll on the income of pastoralist communities and threaten public health security in Mongolia. Mongolian traditional livestock includes sheep, goats, cattle, horses, and camels, and the total livestock number was estimated as 67 million in 2020, which is twenty-two times higher than the human population (National Statistics Office of Mongolia). Livestock in Mongolia are reared under the free-ranging system, and nomadic pastoralists move several times a year searching for water and pasture for their herds. Livestock is the main source of income and food in the pastoralist community, and it produces more than 80% of the agricultural product of Mongolia. However, livestock anthrax cases have been annually

reported since the 1990s, damaging the income of pastoral communities. Human cases are usually reported after the animal incidence.

Despite the current practice involving livestock vaccination, movement control, and disinfecting or burying affected animal carcasses (General Authority for Veterinary Services, 2019), the persistence and frequency of anthrax outbreaks in livestock remain an issue of great concern. Thus, to mitigate anthrax infection, there is a need to design a more prudent control strategy, such as interdisciplinary research with a holistic approach. Furthermore, the global distribution of anthrax demands the convergence of diagnostic technologies to aid detection and surveillance worldwide. However, one major limitation towards achieving anthrax control is the lack of a diagnostic tool devoted to detecting the naturally acquired antibodies of anthrax in animals. Altogether, addressing the problem of anthrax and its associated challenges requires a new approach supported by unprecedented innovations.

This dissertation aims to provide different entry points pertinent to the effective control of anthrax in Mongolia and beyond. In Chapter I, a new ELISA test capable to specifically diagnose anthrax natural infection caused by virulent *B. anthracis* and non-cross reactive to anthrax vaccine-induced antibodies was established to assist anthrax serosurveillance and improve estimates of burden and at-risk populations in Mongolia. In Chapter II, to gain insight into the anthrax epidemiology in Mongolia, spatio-temporal patterns of anthrax in livestock between 1986 and 2015 were analyzed based on the carcass burial sites of animals that died of anthrax in Khuvsgul Province, which showed the highest anthrax incidence rate in Mongolia. The study determined the historical hotspots of carcass sites, places that need to be prioritized in public health intervention, and the factors that precipitate the recurrence of anthrax outbreaks. Moreover, it provided essential epidemiological data that will inform policy and evaluation of current anthrax control measures in Mongolia.

CHAPTER I: Development of ELISA based on *Bacillus anthracis* capsule biosynthesis protein CapA for naturally acquired antibodies against anthrax

Summary

Anthrax is a zoonotic disease caused by the Gram-positive spore-forming bacterium *Bacillus anthracis*. Detecting naturally acquired antibodies against anthrax sublethal exposure in animals is essential for anthrax surveillance and effective control measures. Serological assays based on protective antigen (PA) of *B. anthracis* are mainly used for anthrax surveillance and vaccine evaluation. Although the assay is reliable, it is challenging to distinguish the naturally acquired antibodies from vaccine-induced immunity in animals because PA is cross-reactive to both antibodies. Although additional data on the vaccination history of animals could bypass this problem, such data are not readily accessible in many cases.

In this study, a new enzyme-linked immunosorbent assay (ELISA) specific to antibodies against capsule biosynthesis protein CapA antigen of *B. anthracis*, which is non-cross-reactive to vaccine-induced antibodies in horses was established. Using *in silico* analyses, I screened coding sequences encoded on pXO2 plasmid, which is absent in the veterinary vaccine strain Sterne 34F2 but present in virulent strains of *B. anthracis*. Among the 8 selected antigen candidates, capsule biosynthesis protein CapA (GBAA_RS28240) and peptide ABC transporter substrate-binding protein (GBAA_RS28340) were detected by antibodies in infected horse sera. Of these, CapA has not yet been identified as immunoreactive in other studies to the best of my knowledge. Considering the protein solubility and specificity of *B. anthracis*, the C-terminus region of CapA was prepared, named CapA322, and developed CapA322-ELISA based on a horse model. Comparative analysis of the CapA322-ELISA and PAD1-ELISA (ELISA uses domain one of the PA) showed that CapA322-ELISA could detect anti-CapA antibodies in sera from infected horses but was non-reactive to sera from vaccinated horses. The CapA322-ELISA could contribute to the anthrax surveillance in endemic areas, and two immunoreactive proteins identified in this study could be additives to the improvement of current or future vaccine development.

Introduction

Anthrax is a widely distributed zoonotic disease that occurs in every populated continent (Carlson et al., 2019). After the invention of an effective animal vaccine, outbreaks declined in many parts of the world; however, anthrax remains endemic in some regions of Africa and Asia (Chen et al., 2016; Driciru et al., 2018; Kanankege et al., 2019; Sitali et al., 2018). Anthrax has a substantial economic and public health impact on countries with limited resources to develop anthrax control measures (Vieira et al., 2017). For example, Mongolia is a resource-limited country where anthrax is endemic, except the semi-desert and desert areas in the south (Okutani et al., 2011).

Anthrax is caused by an encapsulated Gram-positive spore-forming bacterium, *Bacillus anthracis*. *B. anthracis* infects a wide range of mammalians, including humans. Herbivores such as antelopes, buffaloes, cattle, sheep, goats, and horses are susceptible to anthrax, whereas birds and canids are comparatively resistant (Mock and Fouet, 2001). The infection occurs in herbivores through browsing, ingestion, or inhalation of a high dose of spores from grazing lands; besides, carnivores are usually exposed through scavenging an infected animal carcass (Hugh-Jones and de Vos, 2002). In addition, the role of tabanid flies and other blood-feeding insects in anthrax transmission in animals has been demonstrated (Ganeva.D.J., 2004; Turell and Knudson, 1987). Humans often acquire anthrax infections from infected animals or materials contaminated with spores, such as wool, hide, and meat (WHO, 2008).

Two plasmids, pXO1 and pXO2, are essential for the virulence of *B. anthracis*. After ingestion or inhalation by the host, spores of *B. anthracis* germinate into vegetative cells that secrete the three pXO1-encoded toxin components: protective antigen (PA), edema factor (EF), and lethal factor (LF). PA is a host cell receptor-binding protein (Mogridge et al., 2002), EF is adenylate cyclase and a potent inhibitor of immune cell function (Leppla, 1982), and LF cleaves mitogen-activated protein kinase and hinders cellular signaling pathways (Duesbery et al., 1998). The pXO2 encodes genes involved in poly-γ-D-glutamic acid (γ-D-PGA), which protects the bacteria from the host phagocytic cells (Drysdale et al., 2005; Jelacic et al., 2014). A lack of either of the plasmids results in a significant loss of virulence of the bacterium (Glinert et al., 2018). The Sterne 34F2 strain, which lacks pXO2 but still secretes the three

major toxin components and retains immunogenicity with less virulence; thus, it is commonly used in anthrax veterinary vaccine production (Turnbull, 1991).

It was previously understood that anthrax mostly resulted in host death; however, field surveys in anthrax-endemic areas have suggested that herbivores infected with a sublethal dose of *B. anthracis* spores could survive (Turnbull et al., 1992). Furthermore, studies have indicated that exposure to a sublethal dose of spores likely elicits adaptive immune responses to *B. anthracis* (Hampson et al., 2011; Lembo et al., 2011). However, the effect of sublethal infection on the adaptive immune response of animals to anthrax is still poorly understood; scaled field studies are needed to detect naturally acquired antibodies in animals.

There is currently no serological test dedicated to distinguishing naturally acquired antibodies against *B. anthracis* from vaccine-induced immunity. Most of the available assays for anthrax serological diagnosis have been developed based on the PA of *B. anthracis* (Marcus et al., 2004; Reuveny et al., 2001). However, due to PA secretion from both naturally virulent and vaccine strains of *B. anthracis*, PA-based assays cannot distinguish the antibodies acquired by vaccination from those acquired by natural infection. So far, additional information such as the vaccination history of herds must differentiate the source of antibodies. However, while anthrax vaccination history is easily obtainable in countries with a good farm management system, accessing such data in developing countries is challenging because of poor record-keeping. For instance, herders in Mongolia have nomadic pastoralism where households migrate to various places to seek pastures for their livestock. Such movements often lead to the loss of important animal records, including vaccination history. In addition, animal identification systems in most local communities are largely uncoordinated, thus complicating the discrimination of vaccinated animals from unvaccinated animals.

Herein, a new enzyme-linked immunosorbent assay (ELISA) test for detecting antibodies against capsule biosynthesis protein CapA of *B. anthracis*, which is non-cross-reactive to vaccine-induced antibodies was developed. First, I screened genes on the pXO2 for ELISA antigen candidates because of the differences between virulent *B. anthracis* ($pXO1^+$, $pXO2^+$) and anthrax vaccine strains ($pXO1^+$, $pXO2^-$). Further, capsule biosynthesis protein CapA (GBAA_RS28240) and peptide ABC transporter substrate-binding protein (GBAA_RS28340) were identified as immunoreactive to hyperimmune horse anti-*B. anthracis* serum. I also found

that the C-terminus region of CapA, named CapA322, is soluble and specific to *B. anthracis*. Therefore, the CapA322-ELISA was developed using the antigen.

Materials and methods

Horse test sera

Hyperimmunized antiserum of horses infected with virulent *B. anthracis* Pasteur No. 1 strain ($pXO1^+$, $pXO2^+$), named PC1 in this study (also known as the Ascoli serum), was obtained from the National Institute of Animal Health, Japan.

Two naturally infected horse sera (PC2 and PC3) were provided by the Institute of Veterinary Medicine of Mongolia. According to records, the two horses showed clinical anthrax symptoms, and *B. anthracis* was isolated from the nasal discharge samples and confirmed with polymerase chain reaction (PCR) (Beyer et al., 1995; Stear, 2005).

To prepare serum samples of vaccinated horses, four 2-year-old female horses (Vac_H1 to Vac_H4) were subcutaneously injected with Sterne vaccine containing 2×10^6 spores/ml, as recommended by the manufacturer (KM Biologics, Japan) at Japan Racing Association. Serum samples were collected before and after vaccination. After vaccination, serum samples were collected every three days starting from day 3 to day 45 postvaccination. Later, samples were obtained every seven days until day 56 postvaccination. The antibody response to PA of *B. anthracis* was evaluated by PAD1-ELISA (Simbotwe et al., 2019). Serum samples with high anti-PA-D1 immunoglobulin G (IgG) titers were obtained on day 21 postvaccination (named Vac_H1D21–Vac_H4D21 for the four horses, respectively) and were used to test the cross-reactivity of CapA322-ELISA.

Two naive horse sera (NC1 and NC2) were purchased from Invitrogen, USA, and KOHJIN BIO, Japan, to serve as negative controls.

Ethical statement

Ethical clearance and research approvals were obtained from the Animal Experiment Committee of Equine Research Institute, Japan Racing Association (Reference: 20-32), and immunization and sampling were conducted according to approved protocols.

In silico analyses

All coding sequences (CDSs) on pXO2 of *B. anthracis* Ames ancestor strain (GenBank accession number: AE017335) were obtained from the National Center for Biotechnology Information and analyzed to predict their cellular localization, secretion, and functional domains. PSORT was used to predict cellular protein localization (Nakai and Horton, 1999), and SignalP was used to predict cleavable N-terminus signal peptide regions (Emanuelsson et al., 2007). Lipoprotein signal peptides identified by LipoP (Juncker et al., 2003), and membrane-associated proteins with transmembrane helix were predicted by the transmembrane-hidden Markov model (TMHMM) algorithm (Krogh et al., 2001). The domains and active sites of the proteins were identified by PROSITE (Hulo et al., 2008). The criteria for selecting candidate genes focused on secreted and surface-exposed CDS products. All CDSs were scored based on the presence of the predicted signal peptide, lipoprotein signal, TMHMM domain, putative domain information, and localization on the cell surface or extracellular secretion. Eight CDSs that scored three or more were selected.

Construction of strains and plasmids

Primers for amplification of candidate CDSs were designed and synthesized by Integrated DNA Technologies (Table 1). Candidate CDSs were amplified from genomic DNA of *B. anthracis* CZC5 (Ohnishi et al., 2014) using KOD FX Neo (TOYOBO, Japan). The vector F (5′-GGGTCGACTCGAGCGGCCGCA-3′) and vector R (5′-GGATCCCAGGGGCCCCTGGAACAG-3′) were used for the linearization of pGEX-6P-2 plasmid, which expresses the glutathione S-transferase (GST) fusion protein. The amplified genes were incorporated into the plasmid using Gibson Assembly (Gibson et al., 2009). The amplified PCR products were analyzed on 1% agarose gel and extracted using the QIAquick Gel Extraction Kit (Qiagen, Germany). The purified fragments with 5′ complementary overhangs were combined in a 1:2 molar ratio of the vector, and the fragments were inserted with 20 μl of Gibson Assembly Master Mix (New England Biolabs, MA, USA) and additional nuclease-free water to obtain a reaction volume of 40 μl. The reaction was then performed at 50°C for 15 min, and the assembled constructs were desalted for an hour using an MF-Millipore membrane filter 0.025 μm (Merck, Germany) on distilled water. *Escherichia coli* 10β (New England Biolabs, MA, USA) was transformed with each construct through electroporation. The

cells and constructs were mixed and transferred to the Bio-Rad 0.1 cm gap Gene Pulser cuvettes. Electroporation was performed using a Gene Pulser Xcell Electroporator (Bio-Rad, CA, USA) set to 1,800 V, 25 μF, and 200 Ω. After electroporation, the cells were immediately transferred to 1 ml of lysogeny broth (LB) and incubated at 37°C for an hour at 180 rpm. Next, 200 μl of the culture was plated on LB agar supplemented with 50 μg/ml ampicillin for selection. The DNA from constructs was purified using a QIAprep Spin Miniprep Kit (Qiagen, Germany), and the sequence of each gene of interest was confirmed by Sanger sequencing using a 3130 xl Genetic Analyzer (Applied Biosystems, MA, USA).

Table 1. Primer list

Primer name	Locus tag	Primer sequence
TZ_F006	GBAA_RS28005	5'-CTGTTCCAGGGGCCCCTGGGATCCATGGCAGCTACACAAGAAACAGCC-3'
TZ_R006		3'-TGCGGCCGCTCGAGTCGACCCTCATCTTGGTACTCTTCGAATTCCTG-5'
TZ_F012	GBAA_RS28035	5'-CTGTTCCAGGGGCCCCTGGGATCCATGGCTACTATGAAAATAAAAGAATGG-3'
TZ_R012		3'-TGCGGCCGCTCGAGTCGACCCTTATCTTCTACGCAATTGATCTGTCC-5'
TZ_F029	GBAA_RS28110	5'-CTGTTCCAGGGGCCCCTGGGATCCATGTGTAAAAGGTTTAAGTTTTTATTGGCTG-3'
TZ_R029		3'-TGCGGCCGCTCGAGTCGACCCTTAATTTGTTTTCTTAAATATATTTTGTTTATTAACG-5'
TZ_F043	GBAA_RS28165	5'-CTGTTCCAGGGGCCCCTGGGATCCATGAACACTAAGGGAATTATAGCAAAAC-3'
TZ_R043		3'-TGCGGCCGCTCGAGTCGACCCTTAGTAATAAGCAGACATGTTATGACCTTTC-5'
TZ_F060	GBAA_RS28240	5'-CTGTTCCAGGGGCCCCTGGGATCCATGAGACGAAAATTGACATTTCAAG-3'
TZ_R060		3'-TGCGGCCGCTCGAGTCGACCCTCAAGTTGTTGTCTCCACTGATAC-5'
TZ_F068	GBAA_RS28275	5'-CTGTTCCAGGGGCCCCTGGGATCCATGAAAATAATAAAATTGTTGATTACATATGG-3'
TZ_R068		3'-TGCGGCCGCTCGAGTCGACCCTATTTAGAAATTACTGTAGCTAGAACACGTTCG-5'
TZ_F083	GBAA_RS28340	5'-CTGTTCCAGGGGCCCCTGGGATCCATGTTAAAAAAAGTAACGCCTATTGTGG-3'
TZ_R083		3'-TGCGGCCGCTCGAGTCGACCCTTATTTCTTCACTTCAGTCCACTTATAG-5'
TZ_F100	GBAA_RS28430	5'-CTGTTCCAGGGGCCCCTGGGATCCATGAAGTATAAAACGCATCTTACAACAAG-3'
TZ_R100		3'-TGCGGCCGCTCGAGTCGACCCTTAACTAAATAACGCTTTAAAGGATTCTAAAAT-5'
TZ_F322	capA322	5'-CTGTTCCAGGGGCCCCTGGGATCCCGTGATAATGGTACTGCAATTCTTG-3'
TZ_R322		3'-TGCGGCCGCTCGAGTCGACCCTCAAGTTGTTGTCTCCACTGATAC-5'

Protein expression and confirmation of immunogenicity

E. coli BL21 cells were transformed with each construct for protein expression. The transformed *E. coli* BL21 cells were grown in 3 ml LB supplemented with 50 μg/ml of ampicillin at 37°C for 18 h at 180 rpm. The OD_{600} of the cultures was adjusted to 0.05 in 3 ml LB or terrific broth (TB) with 50 μg/ml of ampicillin, and the cells were grown at 37°C at 180 rpm. When the OD_{600} reached 0.8, the expression of proteins was induced by adding isopropyl β-D-thiogalactopyranoside (IPTG) to a final concentration of 0.2 mM. The cells were grown at 37°C for 4 h at 180 rpm. In addition, uninduced cell cultures were prepared and used as controls. The cells were harvested at 8,000 rpm for 10 min and washed twice with phosphate-buffered saline (PBS). The cell pellets were resuspended in 250 μl of lysis buffer (PBS containing 0.05% Tween-20, 1 mM PMSF, 0.1 mM benzamidine, pH 7.5) and lysed using a Branson 450 Analog Sonifier (Branson Ultrasonics, CT, USA). The total lysate, supernatant, and pellet fractions of cells were collected. Then, 15 μl of each collected fraction was diluted in 5 μl of sodium dodecyl sulfate (SDS) gel-loading buffer (50 mM Tris-HCl pH 6.8, 2% SDS, 10% glycerol, 1% beta-mercaptoethanol, 12.5 mM EDTA, 0.02% bromophenol blue), and 5 μl of diluted sample was analyzed using 10% SDS polyacrylamide gel electrophoresis (SDS-PAGE).

Detection of expressed GST fusion proteins was achieved by Western blotting using GST Mouse Monoclonal IgG (Santa Cruz, DTX, USA) and anti-mouse IgG-HRP (GE Healthcare, CHI, USA). To identify which proteins were immunoreactive, the hyperimmunized antiserum of horses (PC1) infected with virulent *B. anthracis* strain was used to probe the proteins in the cell pellet fraction, followed by probing with goat anti-horse IgG-HRP (Jackson ImmunoResearch Laboratories Inc, PA, USA) for detection. Upon visualization of the Western blotting, signals of target proteins higher than the background were selected as positive signals.

Expression and purification of CapA322

The peptide derived from the 322^{nd} to the 411^{th} amino acid residues of capsule biosynthesis protein CapA was defined as CapA322. Primers for amplifying partial coding sequence of CapA are described in Table 1, and pGEX-6P-2 was used to construct pTZ006. The protein expression in *E. coli* was conducted using the method described above. After the expression

process, the cells were harvested and lysed using the Branson 450 Analog Sonifier. The resulting suspension was centrifuged at 4°C for 15 min at 15,000 rpm. From the supernatant, GST-tagged recombinant CapA322 was purified using Glutathione Sepharose 4 beads (GE Healthcare, CHI, USA) according to a batch protocol of the manufacturer. The GST tag was cleaved from the protein using the PreScission Protease (GE Healthcare, CHI, USA) at 4°C for 18 h. Then, recombinant CapA322 was eluted with an elution buffer (50 mM Tris, 150 mM NaCl, 1 mM EDTA, 1 mM DTT, pH 7.5). The elution buffer was changed to 25 mM 2-(N-morpholino) ethane sulfonic acid (MES), pH 6.5, using Amicon Ultra centrifugal device (Merck, Germany). After buffer exchange, the collected fraction was loaded onto a Resource-S column (GE Healthcare, CHI, USA) equilibrated with 25 mM MES, pH 6.5. A NaCl gradient from 0 mM to 150 mM was used for elution. The eluted CapA322 protein was stored in aliquots at −80°C. Fractions at all steps of the expression and purification processes were analyzed using 10% SDS-PAGE and Western blotting. For the Western blotting analyses of CapA322, PC1 and NC1 sera were used as primary antibodies, whereas goat anti-horse IgG-HRP was used as a secondary antibody.

CapA322 in-house ELISA

Checkerboard titration was performed to determine the optimal concentration of the reagents (Crowther, 2000). Flat-bottomed 96-well microtiter plates (Corning, NY, USA) were coated with 100 µl per well of serially diluted CapA322 in coating buffer (0.1 M $NaHCO_3$, pH 9.6) and incubated overnight at 4°C. The antigen-coated plates were washed three times with 300 µl wash buffer (PBS containing 0.05% Tween-20, pH 7.4), and the wells were blocked with 100 µl blocking buffer (3% skim milk in PBS containing 0.05% Tween-20, pH 7.4) for 1 h at room temperature (RT). After being briefly washed three times, the sera of PC1 and NC1 were each diluted from 1:100 to 1:6400 in a blocking buffer. Then, 100 µl of the diluted solution was added to wells in triplicate and incubated at RT for 1 h. After being washed again, goat anti-horse IgG-HRP was diluted to 1:15,000 in blocking buffer, and 100 µl of the diluted antibody solution was added to the wells and incubated at RT for 1 h. After washing, an antigen and antibody complex was detected by adding 100 µl 3,3′,5,5′-tetramethylbenzidine substrate (KPL, MD, USA) per well. The reaction was stopped by adding 50 µl 1N HCl per well followed by 20 min incubation at RT. Absorbance at 450 nm (OD 450) was measured using a microtiter plate reader (Thermo Scientific, WI, USA).

Statistical analysis

Each horse serum sample was tested in technical triplicate by PAD1-ELISA and CapA322-ELISA. One sample (Vac_H4D21) did not show the expected antibody response to vaccination when analyzed by PAD1-ELISA, suggesting the failure of immunization. Therefore, this sample was excluded from the following statistical analysis. The rest of the samples were categorized as positive group (PC; n = 3), negative group (NC; n = 2), and vaccinated group (Vac; n = 3). Then, the relative OD values of serum samples were calculated by dividing OD values obtained from PAD1-ELISA by those from CapA322-ELISA. Finally, the one-way ANOVA with Tukey's multiple comparison test was conducted using GraphPad Prism v.7.0 to test for differences among the groups.

Results

Screening of CDS-encoding secreted and surface-associated proteins on pXO2 plasmid.

To select potential antigen candidates among 105 CDSs encoded on pXO2 of *B. anthracis* Ames ancestor strain, *in silico* screening was conducted. Functional features that could make proteins more antigenic were identified by searching for anchoring domain, secretion signal peptide, and cellular localization (Ariel et al., 2002; María et al., 2017).

Five informatics tools were used for the screening. Signal P (Emanuelsson et al., 2007) predicted the product of 12 CDSs to possess the N-terminus signal peptides and secreted through the classical Sec pathway. PSORT (Nakai and Horton, 1999) predicted 2 extracellular proteins, 3 cell wall-associated proteins, 27 cell membrane-related proteins, and 35 cytoplasmic proteins. LipoP (Juncker et al., 2003) predicted 24 proteins: 7 with putative Sec signal peptide SpI sites, 2 with lipoprotein signal peptides SpII sites, and 15 with transmembrane helix domain. TMHMM (Krogh et al., 2001) predicted 33 proteins, including one to six transmembrane helix domains. In addition, PROSITE (Hulo et al., 2008) indicated that several proteins have S-layer homology domains, papain-like cell wall hydrolase domain (NLPC/60), membrane lipoprotein lipid attachment sites, and serine lysine active sites (Table 2).

Table 2. Result of *in silico* analyses on CDSs encoded by pXO2.

CDS	Locus tag	Protein function	SignalP[a]	TMHMM[b]	PSORT[c]	PROSITE[d]	LipoP[e]	Ranking					
								SignalP[a]	TMHMM[b]	PSORT[c]	PROSITE[d]	LipoP[e]	Total score
29	GBAA_RS28110	hypothetical protein	+	1	CMSVM	Prokaryotic membrane lipoprotein lipid attachment site	+	1	1	1	1	1	5
68	GBAA_RS28275	signal peptidase	+	1	CMSVM	Signal peptidases I serine active site		1	1	1	1	0	4
83	GBAA_RS28340	peptide ABC transporter substrate binding protein	+		CWSVM	Prokaryotic membrane lipoprotein lipid attachment site	+	1	0	1	1	1	4
100	GBAA_RS28430	metal dependent hydrolase	+	3	CMSVM			1	1	1	0	0	3
12	GBAA_RS28035	hypothetical protein	+	5	CMSVM			1	1	1	0	0	3
43	GBAA_RS28165	amidase	+		CWSVM	S layer homology domain		1	0	1	1	0	3
60	GBAA_RS28240	Capsule biosynthesis protein CapA	+	1	CMSVM			1	1	1	0	0	3
6	GBAA_RS28005	lysozyme	+	1	ECSVM			1	1	1	0	0	3
3	GBAA_RS27990	hypothetical protein	+	1	Unknown			1	1	0	0	0	2
25	GBAA_RS28090	hypothetical protein	+	1	Unknown			1	1	0	0	0	2
33	GBAA_RS28130	hypothetical protein	+	1	Unknown			1	1	0	0	0	2
9	GBAA_RS28020	hypothetical protein		2	CMSVM			0	1	1	0	0	2
10	GBAA_RS28025	hypothetical protein		1	CMSVM			0	1	1	0	0	2
11	GBAA_RS28030	hypothetical protein		2	CMSVM			0	1	1	0	0	2
16	GBAA_RS28050	hypothetical protein		2	CMSVM			0	1	1	0	0	2
19	GBAA_RS28065	hypothetical protein		2	CMSVM			0	1	1	0	0	2
20	GBAA_RS28070	hypothetical protein		4	CMSVM			0	1	1	0	0	2
21	GBAA_RS28075	hypothetical protein			CMSVM/ CWSVM	Sigma 54 interaction domain ATP binding region A signature		0	0	1	1	0	2
28	GBAA_RS28105	hypothetical protein		1	CMSVM			0	1	1	0	0	2
42	GBAA_RS28160	hypothetical protein		3	CMSVM			0	1	1	0	0	2

50	GBAA_RS28195	CPBP family intramembrane metalloprotease		6	CMSVM		0	1	1	0	0	2
52	GBAA_RS28205	TetR family transcriptional regulator			CMSVM	TetE type HTH domain	0	0	1	1	0	2
54	GBAA_RS28215	undecaprenyl-diphostphatase		2	CMSVM		0	1	1	0	0	2
55	GBAA_RS31175	UDP-diphostphatase		1	CMSVM		0	1	1	0	0	2
61	GBAA_RS28245	poly gamma glutamate biosynthesis protein PgsC		3	CMSVM		0	1	1	0	0	2
62	GBAA_RS28250	poly gamma glutamate synthase PgsB		1	CMSVM		0	1	1	0	0	2
74	GBAA_RS28305	amino acid transporter		6	CMSVM		0	1	1	0	0	2
80	GBAA_RS28325	hypothetical protein		3	CMSVM		0	1	1	0	0	2
81	GBAA_RS28330	CPBP family intramembrane metalloprotease		4	CMSVM		0	1	1	0	0	2
91	GBAA_RS28380	hypothetical protein		1	CMSVM		0	1	1	0	0	2
96	GBAA_RS28405	CPBP family intramembrane metalloprotease		3	CMSVM		0	1	1	0	0	2
98	GBAA_RS31215	hypothetical protein		1	CMSVM		0	1	1	0	0	2
5	GBAA_RS28000	hypothetical protein	+		Unknown		1	0	0	0	0	1
13	GBAA_RS31135	hypothetical protein			CytoSVM	EF hand calcium binding domain	0	0	0	1	0	1
14	GBAA_RS28040	conjugal transfer protein		2	Unknown		0	1	0	0	0	1
18	GBAA_RS28060	hypothetical protein		1	Unknown		0	1	0	0	0	1
23	GBAA_RS28085	hypothetical protein		1	Unknown		0	1	0	0	0	1
38	GBAA_RS28145	hypothetical protein			CMSVM		0	0	1	0	0	1
39	GBAA_RS31155	hypothetical protein		1	Unknown		0	1	0	0	0	1
44	GBAA_RS31160	IS3 family transposase			CytoSVM	Integrase catalytic domain	0	0	0	1	0	1
45	GBAA_RS28180	hypothetical protein		1	Unknown		0	1	0	0	0	1
47	GBAA_RS31165	integrase			Unknown	Endoplasmic reticulum targeting site	0	0	0	1	0	1
53	GBAA_RS28210	IS4 family transposase			Unknown	Sugar transport proteins signature	0	0	0	1	0	1

57	GBAA_RS28225	Capsule synthesis positive regulator AcpB	CytoSVM	PRD domain	0	0	0	1	0	1
59	GBAA_RS28235	Capsule polysaccharide biosynthesis protein	ECSVM		0	0	1	0	0	1
65	GBAA_RS28255	transcriptional regulator	CytoSVM	ArsR type HTH domain type	0	0	0	1	0	1
66	GBAA_RS31190	IS4 family transposase	CMSVM		0	0	1	0	0	1
72	GBAA_RS28295	PRD domain containing protein	CytoSVM	PRD domain	0	0	0	1	0	1
73	GBAA_RS28300	PRD domain containing protein	CytoSVM	PRD domain	0	0	0	1	0	1
76	GBAA_RS28315	Capsule synthesis positive regulator AcpA	CytoSVM	PRD domain	0	0	0	1	0	1
86	GBAA_RS28355	DNA repair protein MucB	CytoSVM	UmuC domain	0	0	0	1	0	1
97	GBAA_RS31210	DNA topoisomerase 3	CytoSVM	Toprim domain and prokaryotic DNA topoisomerase 1 active site	0	0	0	1	0	1
1	GBAA_RS27980	hypothetical protein	CytoSVM		0	0	0	0	0	0
2	GBAA_RS27985	hypothetical protein	Unknown		0	0	0	0	0	0
4	GBAA_RS27995	hypothetical protein	Unknown		0	0	0	0	0	0
7	GBAA_RS28010	ATP binding protein	CytoSVM		0	0	0	0	0	0
8	GBAA_RS28015	hypothetical protein	CytoSVM		0	0	0	0	0	0
15	GBAA_RS28045	hypothetical protein	CytoSVM		0	0	0	0	0	0
17	GBAA_RS28055	hypothetical protein	Unknown		0	0	0	0	0	0
22	GBAA_RS28080	hypothetical protein	Unknown		0	0	0	0	0	0
24	GBAA_RS31140	hypothetical protein	Unknown		0	0	0	0	0	0
26	GBAA_RS28095	hypothetical protein	CytoSVM		0	0	0	0	0	0
27	GBAA_RS28100	hypothetical protein	CytoSVM		0	0	0	0	0	0
30	GBAA_RS28115	hypothetical protein	CytoSVM		0	0	0	0	0	0
31	GBAA_RS28120	hypothetical protein	CytoSVM		0	0	0	0	0	0
32	GBAA_RS28126	hypothetical protein	Unknown		0	0	0	0	0	0
34	GBAA_RS28135	hypothetical protein	CytoSVM		0	0	0	0	0	0
35	GBAA_RS31145	hypothetical protein	Unknown		0	0	0	0	0	0

36	GBAA_RS31150	hypothetical protein	Unknown	0	0	0	0	0	0
37	GBAA_RS28140	hypothetical protein	CytoSVM	0	0	0	0	0	0
40	GBAA_RS28150	parA family protein	CytoSVM	0	0	0	0	0	0
41	GBAA_RS28155	hypothetical protein	Unknown	0	0	0	0	0	0
46	GBAA_RS28185	hypothetical protein	CytoSVM	0	0	0	0	0	0
48	GBAA_RS31170	hypothetical protein	Unknown	0	0	0	0	0	0
49	GBAA_RS28190	hypothetical protein	CytoSVM	0	0	0	0	0	0
51	GBAA_RS28200	DUF523 containing protein	CytoSVM	0	0	0	0	0	0
56	GBAA_RS28220	hypothetical protein	Unknown	0	0	0	0	0	0
58	GBAA_RS28230	DUF1093 domain containing protein	CytoSVM	0	0	0	0	0	0
63	GBAA_RS31180	hypothetical protein	Unknown	0	0	0	0	0	0
64	GBAA_RS31185	hypothetical protein	Unknown	0	0	0	0	0	0
67	GBAA_RS31195	IS6 family transposase	Unknown	0	0	0	0	0	0
69	GBAA_RS28280	hypothetical protein	Unknown	0	0	0	0	0	0
70	GBAA_RS28285	hypothetical protein	CytoSVM	0	0	0	0	0	0
71	GBAA_RS28290	HTH domain containing protein	CytoSVM	0	0	0	0	0	0
75	GBAA_RS29350	hypothetical protein	Unknown	0	0	0	0	0	0
77	GBAA_RS28320	hypothetical protein	Unknown	0	0	0	0	0	0
78	GBAA_RS3144	hypothetical protein	Unknown	0	0	0	0	0	0
79	GBAA_RS31200	hypothetical protein	Unknown	0	0	0	0	0	0
82	GBAA_RS31205	hypothetical protein	Unknown	0	0	0	0	0	0
84	GBAA_RS28345	hypothetical protein	Unknown	0	0	0	0	0	0
85	GBAA_RS28350	DUF3967 domain containing protein	CytoSVM	0	0	0	0	0	0
87	GBAA_RS28360	Yold like family protein	Unknown	0	0	0	0	0	0
88	GBAA_RS28365	hypothetical protein	Unknown	0	0	0	0	0	0
89	GBAA_RS28370	hypothetical protein	CytoSVM	0	0	0	0	0	0

90	GBAA_RS28375	hypothetical protein	CytoSVM	0	0	0	0	0	0
92	GBAA_RS28385	hypothetical protein	Unknown	0	0	0	0	0	0
93	GBAA_RS28390	integrase	CytoSVM	0	0	0	0	0	0
94	GBAA_RS28395	hypothetical protein	Unknown	0	0	0	0	0	0
95	GBAA_RS28400	hypothetical protein	CytoSVM	0	0	0	0	0	0
99	GBAA_RS28425	DUF3991 domain containing protein	CytoSVM	0	0	0	0	0	0
101	GBAA_RS28435	hypothetical protein	CytoSVM	0	0	0	0	0	0
102	GBAA_RS28440	hypothetical protein	CytoSVM	0	0	0	0	0	0
103	GBAA_RS28445	hypothetical protein	Unknown	0	0	0	0	0	0
104	GBAA_RS28450	hypothetical protein	CytoSVM	0	0	0	0	0	0
105	GBAA_RS28455	hypothetical protein	Unknown	0	0	0	0	0	0

[#]Coding sequence

[a] SignaIP: Signal peptide sequences, if detected; +, If not -,

[b]TMHMM: Transmembrane helix domain numbers

[c]PSORT: Putative cell localization of protein

[d]PROSITE: Protein families, domains, and functional sites

[e]LipoP: Lipoprotein signal, if detected; +, If not -,

CMSVM: Membrane protein

CWSVM: Cell wall protein

ECSVM: Extracellular protein

CytoSVM: Cytoplasmic protein

423

I focused mainly on secreted and surface-exposed CDS products that are considered relevant for identifying targets for eliciting protective immunity. Combining the results of the 5 tools, 8 CDSs were selected based on predicted signal sequence, transmembrane helix domain, and cellular localization, considering potential exposure to a host cell and probability to generate host protective response. The candidate proteins were predicted to be secreted, and surface-associated proteins were observed to have 0–5 transmembrane segments (Table 3).

431 **Table 3. *In silico* selected CDSs for identification of immunoreactivity**

Locus tag number	Product name	*In silico* data				
		Cellular localization	Signal peptide[a]	Lipoprotein signal peptide[a]	TMHMM number[b]	Domains and active sites
GBAA_RS28005	Lysozyme	Extra cellular	+	-	1	NlpC/P60
GBAA_RS28035	Hypothetical protein	Membrane	+	+	5	
GBAA_RS28110	Hypothetical protein	Membrane	+	-	1	PROKAR Lipoprotein
GBAA_RS28165	Amidase	Cell wall	+	-	0	SLH
GBAA_RS28240	Capsule biosynthesis protein capA	Membrane	+	-	1	
GBAA_RS28275	Signal peptidase	Membrane	+	-	1	Serine, lysine active sites
GBAA_RS28340	Peptide ABC transport substrate binding protein	Cell wall	+	+	0	PROKAR Lipoprotein
GBAA_RS28430	Metal dependent hydrolase	Membrane	+	-	3	

[a]If secretion or lipoprotein signals were detected; +, If not -,

[b]Transmembrane helix domains

432

Expression and immunoreactivity of candidate proteins

To further identify whether candidate proteins were immunoreactive, the proteins were probed with the hyperimmunized antiserum of horses infected with virulent *B. anthracis* (PC1). CDSs were cloned and expressed in *E. coli*. I successfully constructed *E. coli* strains that express our candidate proteins fused with GST tag at the N-terminus for 5 of 8 CDSs selected from *in silico* analyses (Table 4). The target proteins at the expected molecular sizes were visualized in the lysate, supernatant or pellet fraction of the cell lysate, indicating soluble or insoluble expression (Figure 1). The sizes of the target proteins in the cell pellet fractions were verified using SDS-PAGE (Figure 2A) and Western blotting with antibodies against the GST tag (Figure 2B). After expression verification, proteins were probed with hyperimmune antiserum from horses infected with virulent *B. anthracis* (PC1) to identify their immunoreactivity. Of the 5 expressed proteins, only the capsule biosynthesis protein CapA (GBAA_RS28240) and peptide ABC transporter substrate-binding protein (GBAA_ RS28340) reacted with PC1 serum (Figure 2C). Serum from the naive horse (NC1) showed only background signal with the screened proteins, indicating that the proteins detected using the PC1 serum resulted from an antibody response induced by fully virulent *B. anthracis* infection (Figure 2D).

Table 4. Constructs and strain list

Strain or plasmid	Description	Reference
Plasmids		
pGEX-6P-2	Cloning vector	Reference[1]
pTZ001	pGEX-6P-2 cloned with GBAA_RS28110	This study
pTZ002	pGEX-6P-2 cloned with GBAA_RS28240	This study
pTZ003	pGEX-6P-2 cloned with GBAA_RS28275	This study
pTZ004	pGEX-6P-2 cloned with GBAA_RS28340	This study
pTZ005	pGEX-6P-2 cloned with GBAA_RS28430	This study
pTZ006	pGEX-6P-2 cloned with C-terminus region of GBAA_RS28240	This study
Strains		
E. coli		
BL21	B F^- *ompT gal dcm lon hsdS*$_B$($r_B^-m_B^-$) [$malB^+$] $_{K\text{-}12}$(λ^S)	Reference[2]
BTZ001	BL21 harboring pTZ001	This study
BTZ002	BL21 harboring pTZ002	This study
BTZ003	BL21 harboring pTZ003	This study
BTZ004	BL21 harboring pTZ004	This study
BTZ005	BL21 harboring pTZ005	This study
BTZ006	BL21 harboring pTZ006	This study

[1](Smith and Johnson, 1988)

[2](Jeong et al., 2015)

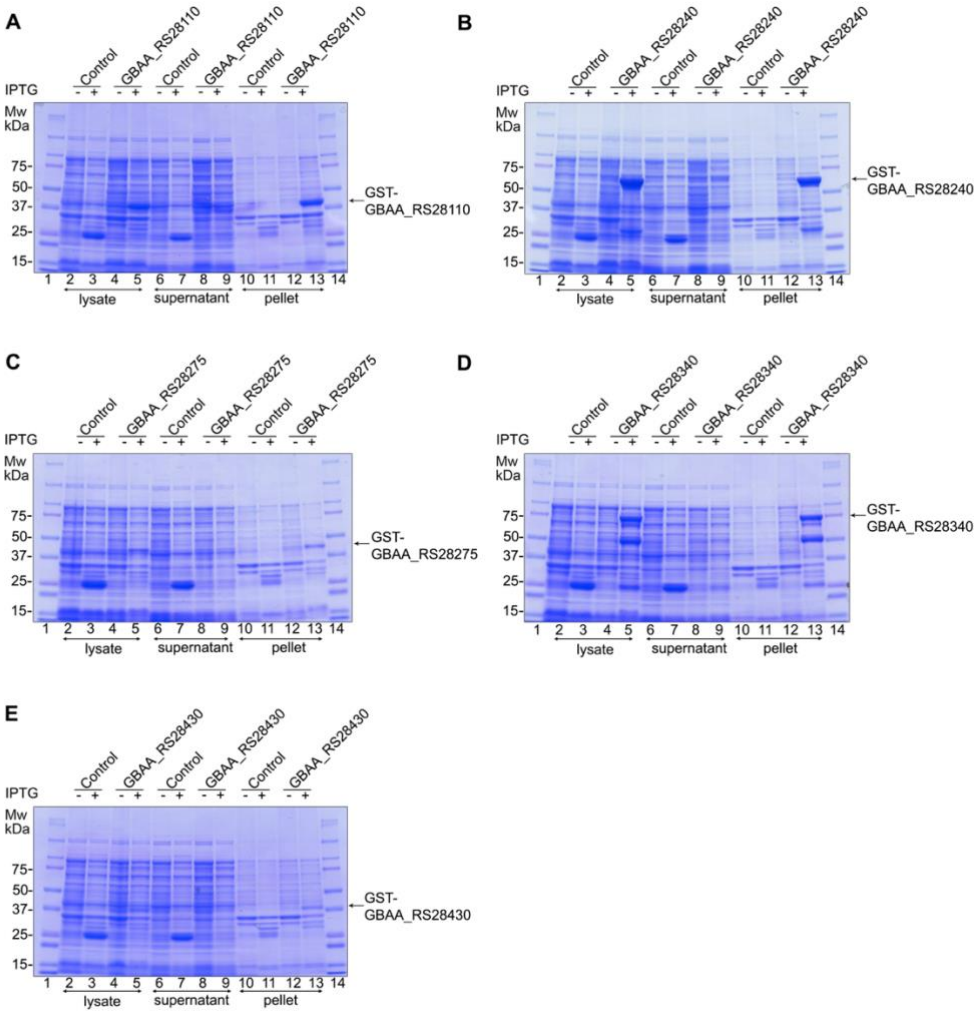

Figure 1. Expression of candidate proteins. Coomassie brilliant blue (CBB) staining analyses of proteins in cell lysate (lanes 2–5), supernatant (lanes 6–9), and pellet (lanes 10–13) fractions of control and candidate protein-expressing *E. coli* strain grown in terrific broth with or without isopropyl β-D-thiogalactopyranoside (IPTG) at 37°C for 4 h at 180 rpm. Lanes 1 and 14, Mw, molecular weight marker (in kDa). Control, *E. coli* BL21 harboring empty pGEX-6P-2 plasmid expressing glutathione S-transferase (GST: 26 kDa). (A) *E. coli* BTZ001 expressing recombinant hypothetical protein (GST-GBAA_RS28110: 44 kDa). (B) *E. coli* BTZ002 expressing recombinant capsule biosynthesis protein CapA (GST-GBAA_RS28240: 72 kDa). (C) *E. coli* BTZ003 expressing recombinant signal peptidase (GST-GBAA_RS28275: 47 kDa). (D) *E. coli* BTZ004 expressing recombinant peptide ABC substrate-binding protein (GST-GBAA_RS28340: 84 kDa). (E) *E. coli* BTZ005 expressing recombinant metal-dependent hydrolase (GST-GBAA_RS28430: 46 kDa). +, 0.2 mM IPTG induction; −, without IPTG induction.

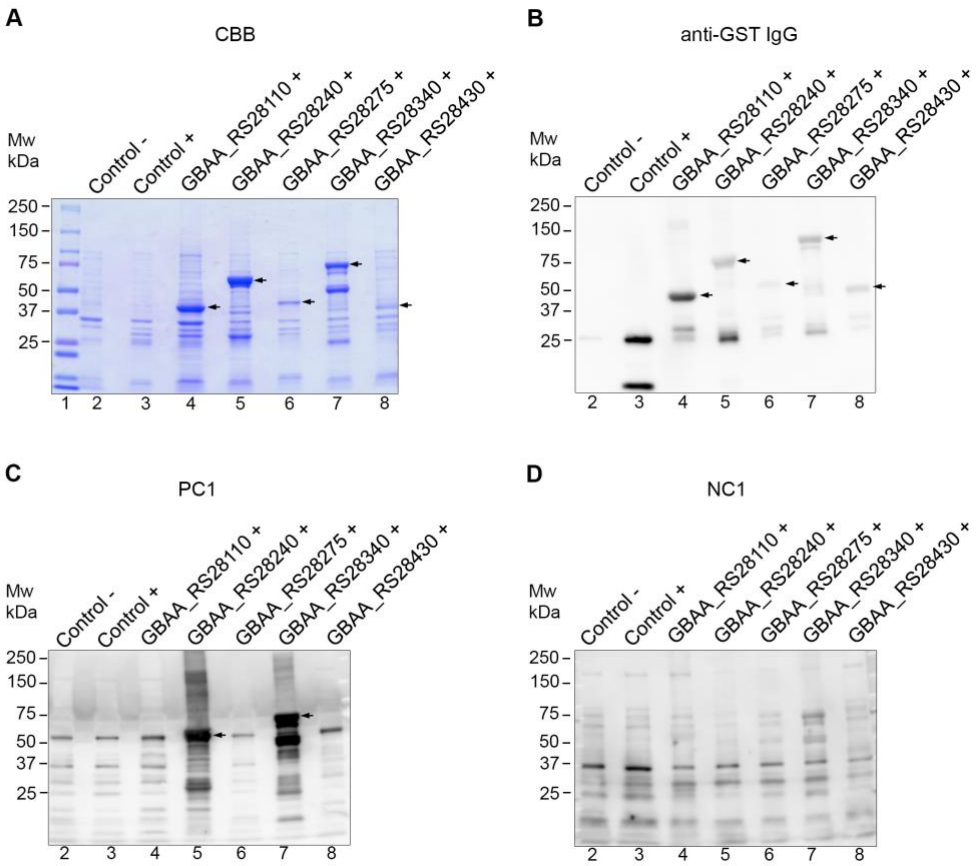

Figure 2. **Expression and immunoreactivity of candidate proteins.** (A) Coomassie brilliant blue (CBB) staining and (B–D) Western blotting of the proteins in cell pellet fractions of the control and candidate protein-expressing *E. coli* strains grown in terrific broth. In Western blotting, the proteins in the cell pellets were probed with different antibodies: (B) anti-glutathione S-transferase (GST) immunoglobulin G; (C) horse hyperimmunized anti-*B. anthracis* serum (PC1); (D) naive horse serum (NC1). Lane 1, Mw, molecular weight marker (in kDa); lane 2, control strain which is *E. coli* BL21 harboring empty pGEX-6P-2 without IPTG induction (-); lane 3, control strain which is *E. coli* BL21 harboring empty pGEX-6P-2 with 0.2 mM IPTG induction (+); lane 4, *E. coli* BTZ001 expressing recombinant hypothetical protein (GST-GBAA_RS28110: 44 kDa); lane 5, *E. coli* BTZ002 expressing recombinant capsule biosynthesis protein CapA (GST-GBAA_RS28240: 72 kDa); lane 6, *E. coli* BTZ003 expressing recombinant signal peptidase (GST-GBAA_RS28275: 47 kDa); lane 7, *E. coli* BTZ004 expressing recombinant peptide ABC substrate-binding protein (GST-GBAA_RS28340: 84 kDa); lane 8, *E. coli* BTZ005 expressing recombinant metal-dependent hydrolase (GST-GBAA_RS28430: 46 kDa). The arrows indicate target proteins in the expected sizes.

Evaluation of CapA322 as ELISA antigen

The sequences specificity of the two proteins, CapA (GBAA_RS28240) and peptide ABC transporter substrate-binding protein (GBAA_RS28340), that showed immunoreactivity to PC1 was analyzed. When the entire length of the proteins was analyzed with tBLASTn, the peptide ABC transporter substrate-binding protein showed high sequence similarity with a protein encoded in *Bacillus cereus*. Alternatively, the CapA showed low sequence similarity to common *B. cereus* strains (~56%) and other *Bacillus* species (55%–60%) evolutionarily related to *B. anthracis*. A few unusual *B. cereus* strains possess virulent plasmids similar (85%–89%) to those of *B. anthracis*, including the toxin and capsule-coding genes (Table 5). Considering the low solubility of whole length CapA, its soluble region at the C-terminus from 322^{nd} to 411^{th} (Figure 3A) was selected. This region also showed even lower sequence similarity (55%) with homologs in common *B. cereus* strains than the N-terminus region. Thus, I tested if the CapA peptide of this region, defined as CapA322, shows better solubility and retains immunoreactivity. The CapA322 was expressed as a GST fusion protein in *E. coli* and solubilized in the supernatant fraction of the cell lysate. The protein size was verified using SDS-PAGE and Western blotting with anti-GST IgG (Figure 3). In GST-tag affinity purification before and after GST-tag cleavage, a GST-CapA322 band of approximately 37 kDa and CapA322 of 11 kDa were detected (Figure 4A). The CapA322 reacted with hyperimmune antiserum from horses infected with virulent *B. anthracis* (PC1) but did not react with serum from the naive horse (NC1) (Figures 4B and 4C). After the first purification process, the remaining host cell derivative contaminants were removed using an ion-exchange chromatography column (Figures 4D and 4E). From a 1L culture, approximately 0.6 mg of CapA322 was obtained with a purity of >90%. As expected, the CapA322 did not react to vaccinated horse serum (Vac_H3D21), which had a high anti-PAD1 IgG concentration (Figure 4F), indicating that the CapA322 is specific to antibodies resulting from virulent *B. anthracis* infection. In addition, its substantial soluble expression confirms that CapA322 is a potent antigen candidate for developing a diagnostic tool.

509 **Table 5. Sequence similarity of two immunoreactive proteins identified by Western**
510 **blotting with horse hyperimmune antisera and CapA322**

Whole length CapA						
ID	Species	Similarity	Positive	Coverage	Plasmid	Chromosome
CP020941.1	*B. cereus* strain BC-AK plasmid pBCXO2	89%	100%	100%	+	
CP001748.1	*B. cereus* biovar anthracis str. CI plasmid pCI-XO2	89%	100%	100%	+	
CP009317.1	*B. cereus* 03BB102 plasmid	86%	96%	94.10%	+	
CP001406.1	*B. cereus* 03BB102 plasmid p03BB102_179	86%	96%	94.10%	+	
CP009636.1	*B. cereus* 03BB108 plasmid pBFI_2	85%	94%	94.10%	+	
CP017574.1	*B. thuringiensis* strain SCG04-02 plasmid PSCG...	57%	79%	93.70%	+	
CP015177.1	*B. thuringiensis* serovar alesti strain BGSC 4...	60%	79%	87.30%	+	
CP023179.1	*B. cereus* strain CC-1	56%	79%	93.60%		+
CP030926.1	*B. butanolivorans* strain PHB-7a	55%	76%	93.90%		+
CP017080.1	*B. muralis* strain G25-68	55%	76%	93.90%		+
CapA322						
ID	Species	Similarity	Positive	Coverage	Plasmid	Chromosome
CP020941.1	*B. cereus* strain BC-AK plasmid pBCXO2	81%	100%	100%	+	
CP001748.1	*B. cereus* biovar anthracis str. CI plasmid pCI-XO2	81%	100%	100%	+	
CP009317.1	*B. cereus* 03BB102 plasmid	91%	95%	73.30%	+	
CP001406.1	*B. cereus* 03BB102 plasmid p03BB102_179	91%	95%	73.30%	+	
CP009636.1	*B. cereus* 03BB108 plasmid pBFI_2	86%	89%	73.30%	+	
CP017704.1	*B. simplex* NBRC 15720 = DSM 1321	59%	86%	70%		+
CP011008.1	*B. simplex* strain SH-B26	60%	84%	70%		+
CP030063.1	*Brevibacterium frigoritolerans* strain ZB201705	57%	84%	70%		+
CP030926.1	*B. butanolivorans* strain PHB-7a	56%	83%	70%		+
CP017080.1	*B. muralis* strain G25-68	57%	76%	70%		+
Peptide ABC substrate-binding protein						
ID	Species	Similarity	Positive	Coverage	Plasmid	Chromosome
CP001748.1	*B. cereus biovar* anthracis str. CI plasmid pCI-XO2	93%	95%	100%	+	
CP020941.1	*B. cereus* strain BC-AK plasmid pBCXO2 sequence	90%	94%	100%	+	
CP015180.1	*B. thuringiensis* serovar alesti strain BGSC 4	90%	94%	100%	+	
DQ025752.1	*B. thuringiensis* serovar kurstaki plasmid pAW	90%	94%	100%	+	
CP018742.1	*B. cereus* strain FORC_047 plasmid pFORC47_2	90%	94%	100%	+	
CP003691.1	*B. thuringiensis* MC28 plasmid pMC183	87%	92%	100%	+	
CP024687.1	*B. wiedmannii* bv. thuringiensis strain FCC41	86%	93%	100%	+	
MG710485.1	*B. thuringiensis* serovar israelensis strain B	86%	92%	100%	+	
CP015154.1	*B. thuringiensis* strain Bc601 plasmid pBTBC4	86%	92%	100%	+	
CP013059.1	*B. thuringiensis* strain YWC2-8 plasmid pYWC2-	86%	92%	100%	+	

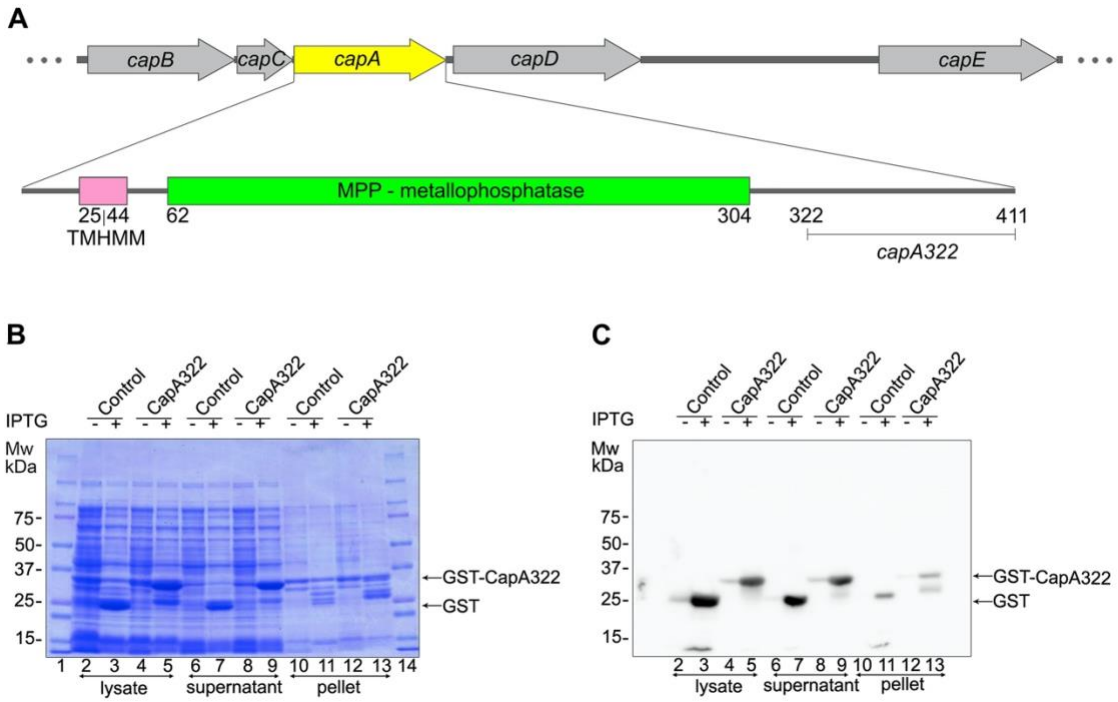

Figure 3. Expression of CapA322. (A) Genetic map of *B. anthracis* capsule-coding operon revealing the CapA322, C-terminus region (amino-acid 322–411) of CapA used in antigen preparation. Coomassie brilliant blue staining (CBB) (B) and Western blotting (C) of proteins in cell lysate (lanes 2–5), supernatant (lanes 6–9), and pellet (lanes 10–13) fractions of control and CapA322 expressing *E. coli* BTZ006 grown in terrific broth with or without isopropyl β-D-thiogalactopyranoside (IPTG) at 37°C for 4 h at 180 rpm. In Western blotting, the proteins were probed with anti-glutathione S-transferase (GST) immunoglobulin G. Lanes 1 and 14, Mw, molecular weight marker (in kDa). Control, *E. coli* BL21 harboring empty pGEX-6P-2 plasmid expressing GST (GST: 26 kDa). BTZ006, *E. coli* expressing recombinant CapA322 (GST-CapA322: 37 kDa). +, 0.2 mM IPTG induction; −, without IPTG induction.

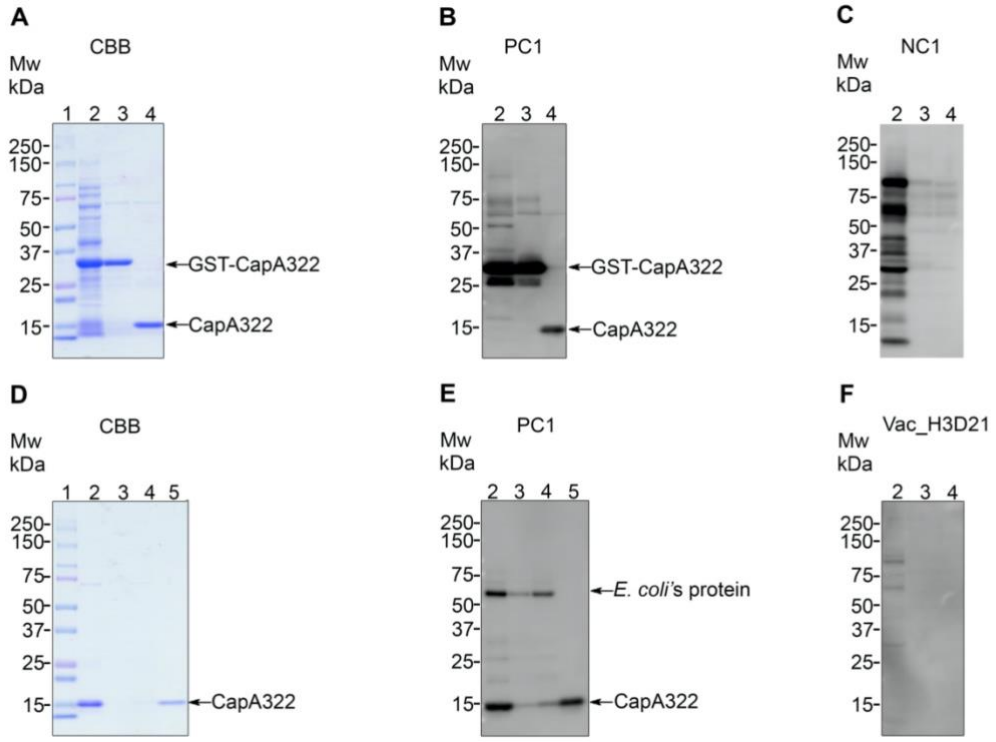

523

524 **Figure 4. Purification of CapA322 from cell culture supernatant.** Coomassie brilliant blue
525 staining (CBB) (A) and (B, C, and F) Western blotting of the fractions collected after affinity
526 batch purification. In Western blotting, proteins were probed with different horse sera: (B)
527 horse hyperimmunized anti-*B. anthracis* serum (PC1); (C) naive horse serum (NC1); (F)
528 vaccinated horse serum (Vac_H3D21). Lane 1, Mw, molecular weight marker (in kDa); lane
529 2, the supernatant fraction applied to affinity beads (GST-CapA322: 37 kDa); lane 3, beads
530 bound; lane 4, elute after treatment with PreScission Protease (CapA322: 11 kDa). (D and E)
531 CBB and Western blotting of the fractions collected during the cation exchange process. Lane
532 1, Mw, molecular weight marker (in kDa); lane 2, sample loaded onto the cation exchange
533 chromatography column; lanes 3 and 4 flow-throughs; lane 5, the eluted protein. Host cell-
534 derived contaminants indicated as *E. coli*'s protein.

Further, to elucidate whether CapA322 is cross-reactive to vaccinated horse serum or not, serum samples from four horses vaccinated with the Sterne vaccine were prepared and the immune responses were evaluated using a PAD1-ELISA (Figure 5A). PA-D1, domain one of the PA of *B. anthracis*, was prepared as previously described (Simbotwe et al., 2019). The optimal titration condition of the PAD1-ELISA for a horse was determined as the PA-D1 antigen concentration of 0.4 μg/ml, serum dilution of 1:100, and a secondary antibody dilution of 15,000 (Figures 5B and 5C). The Sterne vaccine elicited immune responses in three horses out of four starting at 15 days postvaccination. Despite being inoculated with the same dose of vaccine, horses 2 (Vac_H2) and 3 (Vac_H3) showed higher antibody responses than horses 1 (Vac_H1) and 4 (Vac_H4) at all time points. The antibody titers in horses 2 and 3 declined only after the second peak around 5 weeks postvaccination. In contrast, horse 1 showed a weak immune response to the vaccination, with titers decreasing soon after the initial peak. However, horse 4 did not show a detectible immune response despite receiving the same dose of vaccine (Figure 5A).

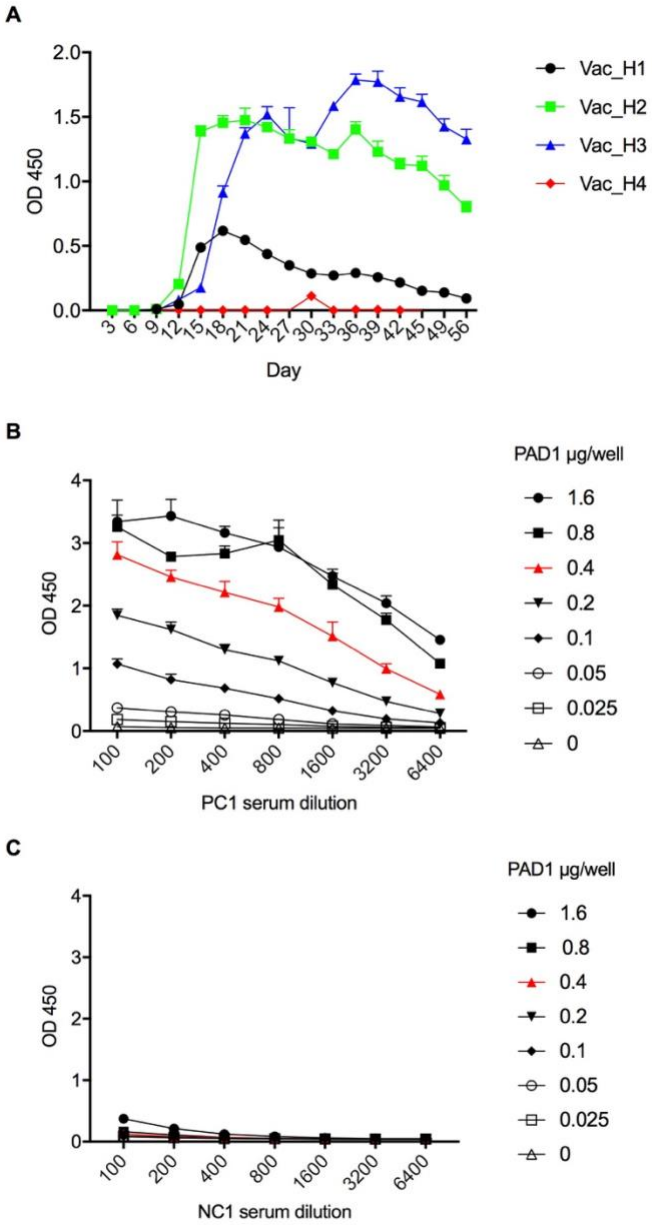

Figure 5. Horses anti-PAD1 immunoglobulin G (IgG) responses against subcutaneously injected *Bacillus anthracis* Sterne 34F2 strain spore vaccine. (A) anti-PAD1 IgG response of vaccinated horses in serum dilution 1:100. Each serum sample was tested in technical triplicate by PAD1-ELISA. Checkerboard titration between PAD1 and (B) horse hyperimmunized anti-*B. anthracis* serum (PC1) or (C) naive horse serum (NC1) in PAD1-ELISA. Each dilution of serum sample was tested in technical triplicate. The twofold serum dilution starts with a dilution of 1:100, and PAD1 dilution starts with 1.6 µg/well. From the result, the optimal concentrations of the antigen, antibody, and serum dilutions were determined as follows: antigen, 0.4 µg/well; serum dilution, 1:100; second antibody dilution, 1:15,000.

CapA322-ELISA and PAD1-ELISA

Based on the CapA322 antigen, the CapA322-ELISA was developed. An antigen concentration of 0.8 μg/ml, serum dilution of 1:100, and a secondary antibody dilution of 15,000 were determined as the optimal titration conditions of CapA322-ELISA for horses (Figures 6A and 6B). Each serum sample from horses experimentally (PC1) or naturally infected with virulent *B. anthracis* (PC2 and PC3) and horses immunized with Sterne vaccine (Vac_H1D21-Vac_H4D21) as well as naive horses (NC1 and NC2) was technically triplicated and comparatively tested by the CapA322-ELISA and PAD1-ELISA (Figure 6C). As expected, PC1 and PC2 gave a significantly higher OD absorbance than the NC1 and NC2 in both CapA322 and PAD1-ELISAs. Vaccinated horse sera Vac_H1D21–Vac_H3D21 showed high OD absorbance in PAD1-ELISA, whereas all were negative in CapA322-ELISA. However, the PC3 serum exhibited a positive reaction only with CapA322-ELISA but was negative in PAD1-ELISA.

Furthermore, except one sample (PC3), relative OD values in group PC were around 1, suggesting that the two tests (PAD1-ELISA and CapA322-ELISA) were comparable in detecting virulent *B. anthracis* infection. Similarly, relative OD values in group NC were around 1, indicating that the two tests give the same result. However, relative OD values in group Vac ranged from 13.0 to 39.9, showing the non-cross reactivity of CapA322-ELISA with vaccine-induced antibodies. This result was supported by the observation that the relative OD values in vaccinated group were significantly higher than those in the positive ($p = 0.03$) and negative ($p = 0.04$) groups (Figure 6D).

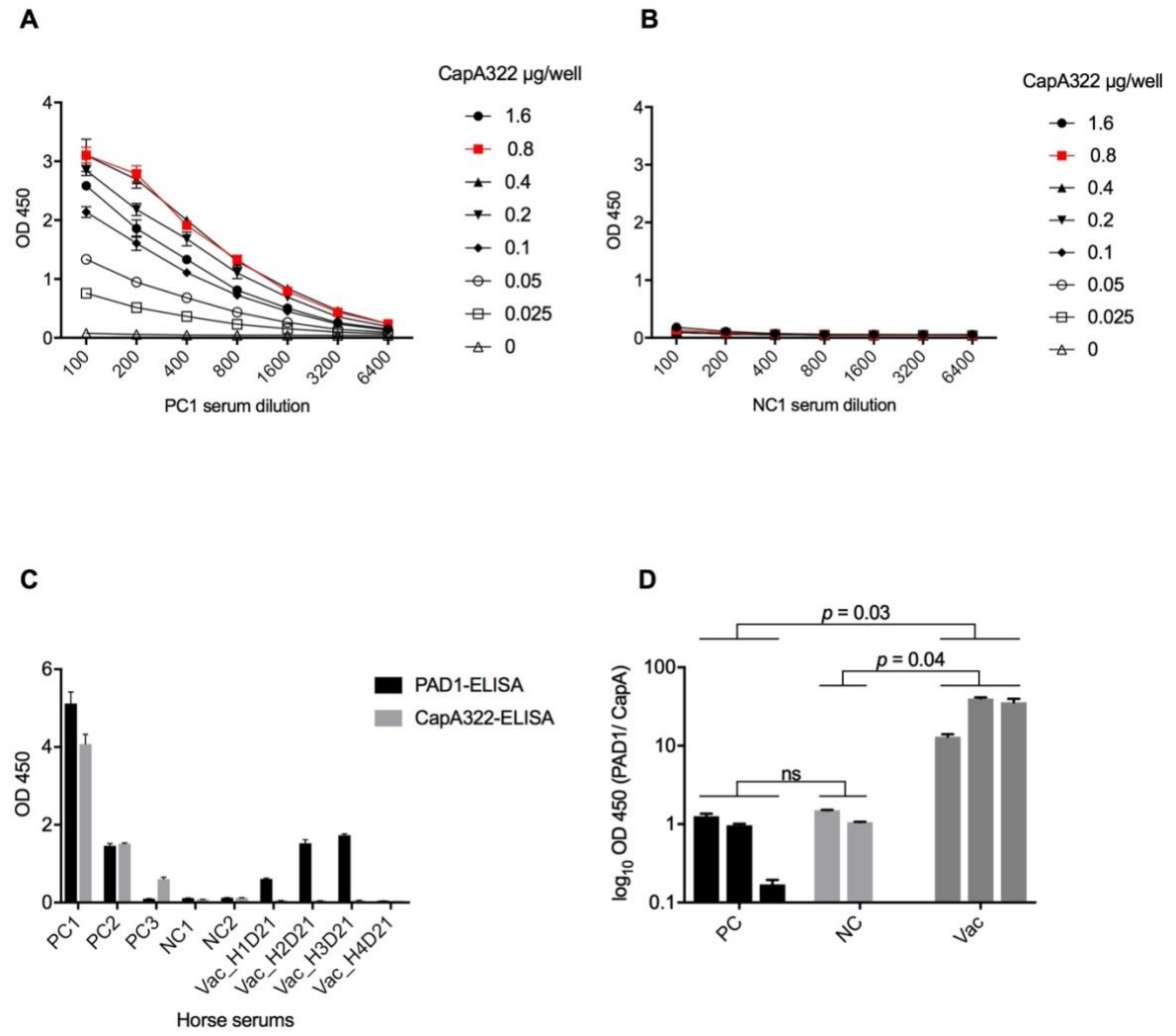

Figure 6. Comparison of PAD1-ELISA and CapA322-ELISA. Checkerboard titration between CapA322 and (A) horse hyperimmunized anti-*Bacillus anthracis* serum (PC1) or (B) naive horse serum (NC1) in CapA322-ELISA. Each dilution of serum sample was tested in technical triplicate by CapA322-ELISA. The twofold serum dilution starts with a dilution of 1:100, and CapA322 dilution starts with 1.6 µg/well. From the result, the optimal concentrations of antigen, antibody, and serum dilutions were determined as follows: antigen, 0.8 µg/well; serum dilution, 1:100; second antibody dilution, 1:15,000. (C) Comparison of PAD1-ELISA and CapA322-ELISA on horse sera. Each serum samples of horse hyperimmunized anti-Bacillus anthracis (PC1), horse naturally infected with *B. anthracis* (PC2 and PC3), naive horses (NC1 and NC2), and horse vaccinated with Sterne34F2 strain (Vac_H1D21-Vac_H4D21) was analyzed in technical triplicate by PAD1-ELISA and CapA322-ELISA. (D) One-way ANOVA with Tukey's multiple comparison test on relative OD values of positive (PC; n = 3), negative (NC; n = 2), and vaccinated (Vac; n = 3) groups.

Discussion

In this study, potential antigen candidates encoded by pXO2 were screened by *in silico* analyses, and the CapA322-ELISA was developed to detect antibodies against CapA, which is secreted from virulent *B. anthracis* strains that possess pXO2.

Identifying the *B. anthracis* natural infection, specifically sublethal infection in animals, is vital in predicting outbreaks in endemic areas. Additionally, identifying sublethal infection can also aid in describing anthrax dynamics in ecosystems and understanding the host-pathogen interaction, which is still poorly understood (Carlson et al., 2018). Current conventional serological assays for anthrax diagnosis and evaluation of immune responses to anthrax vaccines have been developed based on the PA of *B. anthracis*, which is reactive to both naturally acquired and vaccine-generated antibodies. Though animals with natural infections could be distinguished from vaccinated animals based on vaccination history, collecting such data is somewhat cumbersome due to data accessibility and missing records. Besides, although the duration of solid immunity among vaccinated animals is no longer than a year (Stear, 2005), a previous study found that residual antibodies in vaccinated animals were still significantly higher than non-vaccinated animals even after a year had passed (Simbotwe et al., 2019). Given the importance of serodiagnosis for distinguishing *B. anthracis* natural infection from vaccine immunity, the CapA322-ELISA that detects antibodies against CapA encoded by pXO2 of *B. anthracis* without cross-reacting with sera from vaccinated animals (Figures 4F and 6C) was developed.

Except for a few unusual *B. cereus* strains (Table 5), the C-terminus region of CapA, named CapA322, has lower sequence similarity with other bacterial species and showed immunoreactivity with sera from horses infected with virulent *B. anthracis*. The γ-D-PGA capsule of *B. anthracis*, a critical virulence determinant of *B. anthracis*, is synthesized by CapB and CapC, and transported by CapA and CapE across the cell membrane (Candela and Fouet, 2005). Thus, CapA is essential for transporting the γ-D-PGA, but the immunoreactivity of this membrane protein is yet to be determined. To the best of our knowledge, this study is the first to identify CapA as immunoreactive. While the whole length of CapA, as well as its C-terminal region (CapA322), are immunoreactive (Figure 4B), the CapA322 was selected for ELISA

development because it was more soluble (Figure 3) compared to the whole length protein (Figures 1 and 2A).

CapA is a single-pass transmembrane protein that belongs to the metallophosphatase superfamily (Lu et al., 2020). A single transmembrane helix domain is located at the N-terminus region from 25 to 44 of CapA, translocating the protein in the cell membrane, thereby exposing the C-terminus region to the cell exterior. This exposed cell surface can define the immunoreactive characteristic of the CapA322. Many antigens or vaccine candidate-searching studies have been targeting surface-exposed proteins (Chakravarti et al., 2000; Pizza et al., 2000; Sutcliffe and Harrington, 2002). Cell surface molecules have a greater chance to generate a host cell immune response by its position as they are more exposed to host cells (Chaudhuri et al., 2014). Previously, a few unusual *B. cereus* strains have been reported to cause anthrax-like disease in animals and humans due to the acquisition of virulence plasmids that are highly similar to the *B. anthracis* virulence plasmids pXO1 and pXO2 (Hoffmaster et al., 2006; Klee et al., 2010). Those *B. cereus* strains are divided into two variants; atypical strains such as 03BB102 and 03BB108 and *B. cereus* biovar anthracis (Bcbva) strains such as BC-AK and CI (Baldwin, 2020). *B. anthracis* CapA exhibited relatively high sequence homology with the so-called Bcbva and atypical *B. cereus* strains (Table 5); therefore, it is possible for CapA322-ELISA to cross-react with such strains. However, these strains have only been reported in rare cases (Cachat et al., 2008; Han et al., 2006; Sergeev et al., 2006). Also, studies suggest that pXO2 plasmid is not commonly distributed in *B. cereus* and *B. thuringiensis* strains, which are closely related to *B. anthracis* (Kim et al., 2005; Ramisse et al., 1996). Moreover, screening of pXO2 ORFs among *B. cereus* group strains revealed a restricted distribution of *cap* genes other than in *B. anthracis* (Pannucci et al., 2002). Further, despite the presence of *cap* genes, it is doubtful whether *cap* genes in atypical *B. cereus* strains 03BB102 and 03BB108 are expressed because there was no capsule expression detected in-vitro conditions where it is normally expressed in *B. anthracis* (Cachat et al., 2008; Hoffmaster et al., 2006). A part of the plasmid harbored by strain 03BB102 is highly similar to a portion of the *B. anthracis* pXO2, but the rest of the sequence is different (Baldwin, 2020); therefore, *cap* genes expression might be attenuated in this strain, resulting in the absence of capsule. Although CapA homologs in Bcbva and atypical *B. cereus* strains are not expected to significantly confound the result of CapA322-ELISA because of the rarity of such strains in nature, further validation is required to examine the specificity of CapA322-ELISA by assessing possible antibody cross-reactivity.

A comparison of results from CapA322-ELISA and PAD1-ELISA showed that CapA322-ELISA could detect anti-CapA antibodies in the sera of horses experimentally and naturally infected with virulent *B. anthracis* strains. Several ELISAs have been used for serodiagnosis of *B. anthracis* infection, including assays for detecting anti-LF (Ghosh et al., 2013) and PA (Ghosh and Goel, 2012) IgGs; however, detected antibodies themselves are insufficient to distinguish the natural infection of *B. anthracis* from vaccine immunity. Moreover, there is an ELISA for detecting anti-γ-D-PGA IgG of *B. anthracis* (Harrison et al., 1989). However, Chen *Z et al*. found γ-D-PGA antibodies in sera of *B. anthracis* non-infected chimpanzees (n = 9) and humans (n = 6), which were likely the result of exposure to other *Bacillus* species (Chen et al., 2015). In our study, anti-CapA antibodies were not detected in any horse sera (n = 6) other than positive samples (n = 3) when the starting dilution of 1:100 was used (Figure 6C). In addition, unlike PA-based ELISA, CapA322-ELISA showed an advantage of non-cross-reactivity with vaccinated horse sera, suggesting that the CapA322 can be a helpful tool for determining the naturally acquired immune response of animals. For further validation of the CapA322-ELISA, screening a larger sample size for horses, including cattle, is needed. Future work will therefore include follow-up work designed to validate the assay.

In preparing vaccinated horse serum samples, significant diversity in the antibody response was observed (Figure 5A). This is in line with data observed by Phaswana *et al*. (Phaswana et al., 2017) where five individual Boer goats vaccinated with Sterne 34F2 *B. anthracis* strain showed variable levels of immune response. The Sterne vaccine elicited an immune response in three out of four vaccinated horses in our study. However, the anti-PA IgG titers progressively declined from around 5 weeks postvaccination (Figure 5A). This could explain the negative result observed when the serum of PC3 collected from *B. anthracis* naturally infected horse was tested by PAD1-ELISA (Figure 6C). Although the time interval from infection to sample collection could not be determined, it can be speculated that the anti-PA IgG titer in PC3 serum had already decreased below detectible levels by that time. Also, as a major limitation of this study, weekly anti-PA IgG titers in PC2 and PC3 could not be evaluated as these were collected at a single point in time and analyzed retrospectively. Nevertheless, the anti-CapA antibodies were detectable by our developed assay, suggesting better stability relative to anti-PA IgG. Although the horses were carefully selected as the same age and sex and subcutaneously vaccinated them with the same lot of vaccines using the same procedure, one horse did not show any immune response (Figure 5A). Therefore, this observation may

have been due to differences in the horse's immunological state or genetic background rather than technical vaccination failure. Therefore, more studies with various vaccine doses and challenging tasks will be needed to determine the optimal amount for horse vaccination.

In addition to the CapA (GBAA_RS28240), peptide ABC transporter substrate-binding protein (GBAA_RS28340) was identified as immunoreactive. The peptide ABC transporter substrate-binding protein was previously reported to be seroreactive with antisera of rabbit and mice infected with *B. anthracis* Ames spore, and convalescent serum from rhesus macaques vaccinated with Anthrax Vaccine Adsorbed (AVA, BioThrax) (McWilliams et al., 2012). Chitlaru T *et al*. (Chitlaru et al., 2007) highlighted that substrate-binding proteins of ABC transporters are highly immunogenic protein classes. It also noteworthy that Orit Gat *et al.* conducted a similar study in search of potential immunogen proteins from the *B. anthracis* genome, including two virulence plasmids. Three of their eight selected proteins from pXO2, lysozyme (GBAA_RS28005), amidase (GBAA_RS28165), and metal-dependent hydrolase (GBAA_RS28430), coincided with our selection. Although I failed to clone CDSs of lysozyme (GBAA_RS28005) and amidase (GBAA_RS28165), they determined that these two proteins are immunoreactive with guinea pig and rabbit hyperimmunized with Vollum strain of *B. anthracis* ($pXO1^+$, $pXO2^+$) (Gat et al., 2006). In contrast, metal-dependent hydrolase (GBAA_RS28430) was negative, which was the same as our result. The immunoreactive proteins identified here and in previous studies (Ariel et al., 2002; Chitlaru et al., 2007; Gat et al., 2006; Kempsell et al., 2015; McWilliams et al., 2012) may be the first candidates for future diagnostic developments. These proteins may provide valuable additives for AVA improvement; the vaccine is currently licensed for humans and consists primarily of PA (Turnbull et al., 1986). Although the vaccine is effective, expanding the vaccine protection by including additional antigens in its formulation is necessary for a less demanding vaccination regimen and as a defense against bioterrorism (Grabenstein, 2008). Further, regardless of the protective immunity provided by PA, previous studies noted that relying on antibodies against PA as the sole protector against anthrax is unconvincing due to the variable protection level conferred by antibodies generated by the PA-based vaccine (Ivins et al., 1995; Ivins et al., 1998; Ivins et al., 1992; Welkos and Friedlander, 1988). Our study showed the possibility of antibodies against PA being short-lived in the sera of vaccinated animals, which declined to range from 3 to 5 weeks after immunization (Figure 5A). Considering these aspects, adding recombinant antigens to the PA might increase the durability and protective efficacy of the

AVA vaccine with a less demanding vaccination regimen through a multi-antigen cocktail vaccine, as has been achieved against *Bordetella pertussis* infection (Jefferson et al., 2003).

CHAPTER II: Risk Factors and Spatio-temporal Patterns of Livestock Anthrax in Khuvsgul Province, Mongolia

Summary

Anthrax, a worldwide zoonotic disease, has long been a public health and socio-economic issue in Mongolia. Presently, there is no spatial information on carcass burial sites as a potential hazard of future anthrax outbreaks and possible risk factors associated with anthrax occurrences in Mongolia.

Here, retrospective data (1986–2015) on the disposal sites of livestock carcasses was analyzed to describe historical spatio-temporal patterns of livestock anthrax in Khuvsgul Province, which showed the highest anthrax incidence rate in Mongolia. From the results of spatial mean and standard deviational ellipse analyses, the study found that the anthrax spatial distribution in livestock did not change over the study period, indicating a localized source of exposure. The multi-distance spatial cluster analysis showed that carcass sites distributed in the study area are clustered. Using kernel density estimation analysis on carcass sites, two anthrax hotspots were identified in low-lying areas around the south and north regions. Notably, this study disclosed a new hotspot in the northern part that emerged in the last decade of the 30-year study period. The highest proportion of cases was recorded in cattle, whose prevalence per area was highest in six districts (i.e., Murun, Chandmani-Undur, Khatgal, Ikh-Uul, Tosontsengel, and Tsagaan-Uul), suggesting that vaccination should prioritize cattle in these districts. Furthermore, size of outbreaks was influenced by the annual summer mean air temperature of Khuvsgul Province, probably by affecting the permafrost freeze-thawing activity.

Introduction

Anthrax is a zoonotic disease caused by the Gram-positive bacterium *Bacillus anthracis*, existing as a spore outside its host animal (Mock and Fouet, 2001). The spores are highly resistant to extreme temperatures, radiation, and chemical substances and can persist in soil for several decades (Stephens, 1998). Anthrax has a wide range of mammalian hosts, including humans, livestock, and wildlife. Domesticated herbivores such as cattle, sheep, and goats are the most susceptible to anthrax; grazing with ingesting or inhaling high doses of spores usually culminates in fatal disease (Hugh-Jones and de Vos, 2002). Anthrax is not contagious as direct transmissions between herbivores are thought to be rare (Beyer and Turnbull, 2009; Fasanella et al., 2010). Although herbivores are the primary hosts for anthrax, humans also get infected with anthrax through contact with infected animals or contaminated animal products, such as meat, hide, and wool (Kaufmann and Dannenberg, 2002).

Several environmental factors influence the persistence of *B. anthracis* spores and the onset of anthrax outbreaks. Long-range dispersal of spores is influenced by weather conditions, such as floods and strong winds (Fox et al., 1977; Munang'andu et al., 2012), and by biological vectors, such as birds, scavengers, and biting flies (Cieslak and Eitzen, 1999; Dragon et al., 2001; Turell and Knudson, 1987). Soil conditions, such as high moisture, rich calcium, high organic content, and pH neutral to alkaline, correlate with the onset of outbreaks (Dragon and Rennie, 1995; Hugh-Jones and Blackburn, 2009). Spores can be concentrated in low-lying areas through runaway by rain and water streams, affecting the spatial distribution of outbreaks (Van Ness, 1971). Recent studies highlight the role of permafrost in preserving *B. anthracis* spores for a long time in the frozen ground below 0 °C, and the effect of increasing temperature on permafrost thawing due to the spore spillover to the soil surface (Timofeev et al., 2019).

Anthrax is globally distributed, and sporadic cases have been reported on every populated continent (Carlson et al., 2019). In industrialized countries where focused, comprehensive, and sustained livestock vaccination programs have been successfully implemented, the disease has dramatically declined (Hampson et al., 2011). However, the burden of anthrax remains high in low- and middle-income countries in Africa and Asia, where animal vaccination is erratic (Vieira et al., 2017).

In Mongolia, anthrax has posed severe challenges to public health and veterinary services for a long time. Approximately 25% of the national population of 3,000,000 residents live a nomadic pastoral lifestyle, raising livestock under a free-ranging system. Livestock products are an essential income source for these people (Shagdar, 2002), thus, making anthrax control a great priority. Mongolia was once a socialist country with close connections to the Soviet Union from around 1920 to the late 1980s. The introduction of routine animal vaccination from 1948 onward resulted in a drastic decrease in anthrax incidence (Odontsetseg et al., 2007). However, following the collapse of the Soviet Union, political revolution and economic transition from socialism to a free market began in the early 1990s in Mongolia. Due to the transformation recession, healthcare delivery and mass vaccination in the veterinary sector were ceased (Ebright et al., 2003). Among 19 of 21 provinces in Mongolia, with records of anthrax incidences, frequent outbreaks are restricted to the provinces at the northern and northeastern regions of the country (Odontsetseg et al., 2007). Among them, Khuvsgul has the highest livestock anthrax rate, accounting for 40.35% of all cases (Badmaeva et al., 2014).

The spores of *B. anthracis* can persist in soil for several decades, and may even be preserved longer in frozen grounds (Stella et al., 2020). The potential hazard of the historic carcass sites was confirmed by surveys of viable spore detection in previous carcass sites (Dragon et al., 2001). The current disposal practice of animals dying from anthrax in Mongolia mainly involves burying, and those carcass burial grounds are generally identical to outbreak locations (General Authority for Veterinary Services, 2019). Although disease control measures include restriction of access to carcass burial sites, which are most likely to be contaminated with spores, presently, there is a lack of information on the spatial pattern of carcass sites, thus limiting the implementation of interventions. Here, retrospective data (1986–2015) on the burial sites of livestock carcasses was analyzed to describe historical spatial patterns and temporal trends in livestock anthrax across the Khuvsgul Province to answer the following questions; What is the spatial pattern of carcass sites? Where are the areas of high carcass site concentration in previous and recent times? Which districts have more burden of anthrax? Also, The study was interested in exploring the relationship between the number of anthrax cases and animal population, annual mean precipitation, and annual mean summer air temperature, considering the anthrax seasonality in Mongolia (Odontsetseg et al., 2007). This study is the first spatio-temporal study on anthrax in Mongolia and could serve as a baseline for future anthrax studies and public health interventions.

Materials and methods

Data source

Among 21 administrative provinces in Mongolia, Khuvsgul Province is the northmost province, bordering Siberia, Russia, with 24 districts. Anthrax is notifiable under the law on Livestock Health and Gene Protection of Mongolia (General Authority for Veterinary Services, 2019). Thus, reporting all suspected cases of anthrax is mandatory. An animal or animal carcass with symptoms suggestive of anthrax (e.g., high fever, breathing difficulty, sudden death, a carcass without rigor mortis, etc.) was considered as a suspicious case, while a positive standard bacteriology and/or molecular laboratory tests was defined as a confirmed case (Stear, 2005). Here, basic yearly information on livestock in Khuvsgul Province, including livestock and human population, the number of livestock anthrax cases, and GIS data of carcass burial sites from 1986 to 2015 were collected. The Department of Veterinary Services of Khuvsgul Province, Mongolia, provided the geographic information system (GIS) data for anthrax carcass disposal sites recorded between 1986 and 2015. All these sites represent confirmed cases previously diagnosed by clinical examination and standard bacteriology method at the local veterinarian and the State Central Veterinary Laboratory (SCVL), Ulaanbaatar, Mongolia. The standard bacteriology methods included Giemsa and polychrome methylene blue (PMB) staining for microscopic detection of *B. anthracis* and its poly-D-glutamic acid capsule in blood smears. The methods also involved culture and isolation of the bacterium, as previously described in the OIE manual (Stear, 2005). In addition, samples collected after 2000 were further confirmed by polymerase chain reaction (PCR) for the detection of toxin (*pagA*) and capsule (*capB*) coding genes of *B. anthracis* at the SCVL. This improvement in disease diagnosis would not significantly impact the anthrax surveillance since the disagreement between the standard bacteriology and PCR tests for anthrax confirmation is negligible (Beradze, 2019).

The livestock and human population data in the Khuvsgul Province was obtained from the Statistics Office of Khuvsgul Province, Mongolia (National Statistics Office of Mongolia). Data on annual precipitation and air temperature of Khuvsgul Province were provided by the Information and Research Institute of Meteorology, Hydrology, and Environment, Mongolia. Administrative areas, elevation, and inland water maps of Mongolia were downloaded from

the database of DIVA-GIS (Hijmans et al., 2004). The project was approved by the review board of the Institute of Veterinary Medicine, Mongolia, Reference number: 20082001.

The cattle anthrax prevalence per area in Khuvsgul Province by districts (1986–2015)

The annual average prevalence of anthrax per 1,000,000 cattle population per 1000 km^2 was calculated at the district level. *B. anthracis* is a non-invasive pathogen regarded as non-contagious; therefore, direct animal-to-animal transmission is not expected to occur except in osteophagia or carnivore activities (Beyer and Turnbull, 2009; WHO, 2008). Indeed, soil is the natural reservoir of the *B. anthracis* spores and becomes the primary source of animal infection (Carlson et al., 2018). Thus, considering the mode of anthrax transmission, the cattle anthrax prevalence was estimated, taking into account the area (km^2) of each district as follows:

$$prevalence\ per\ area = \frac{annual\ average\ anthrax\ cases}{(average\ animal\ population \times area)}$$

A cartographic map was used to visualize the distribution of cattle anthrax prevalence using ArcGIS v.10.6.1 (ESRI Inc., Redlands, CA, USA).

The spatial mean and standard deviational ellipse analyses

The analyses were conducted on ArcGIS v.10.6.1 software (ESRI Inc., Redlands, CA, USA) (Environmental Systems Research Institute). The standard deviational ellipse (SDE) analysis was performed to summarize the spatial attributes of geographic features with coordinates (Yuill, 1971). The unweighted spatial mean and SDE analyses were used to determine the directional trend and spatial characteristics of carcass sites in the study area. To reveal the temporal changes of carcass sites resulting from anthrax incidences, the entire study period was divided into three time parts: 1986–1995, 1996–2005, and 2006–2015.

Multi-distance spatial cluster analysis

According to the guide on the manufacturer's website, a multi-distance spatial cluster analysis tool in ArcGIS v.10.6.1 software (ESRI Inc., Redlands, CA, USA) was used to

determine the maximum distance relationship between animal carcass sites (Environmental Systems Research Institute). The tool uses Ripley's K function as shown in the equation

$$L(d) = \sqrt{\left[A \sum_{i=1}^{N} \sum_{j=1, i \neq j}^{N} k(i,j)\right] / [\pi N(N-1)]}$$

where d is the distance, N is the total number of events, A is the area, and the weight k(i, j) is the influence of the elements within the distance. When the distance between i and j is less than or equal to d, k(i, j) is 1, and k(i, j) is 0 when the distance between i and j is greater than d.

To analyze the spatial pattern of carcass sites, observed K-values, determined using actual GIS coordinates, were compared with the expected K-values, calculated through the random spatial distribution of carcass sites. The defaults 10 times was used as the number of distance changes with 999 simulations, equal to confidence levels of 99.9%. The minimum enclosing rectangle was utilized as the study area method. Positive value from the difference between the observed K and expected K (Diff K) indicates clustering. When the observed K-value for a specified expected K-value is larger than the upper confidence envelope (HiConEnv) value, the spatial value is statistically significant. In the following kernel density estimation analysis, to avoid underestimating the hotspot areas, the maximum expected K with a statistically significant value was used as the maximum distance for the relationship between carcass sites in the Khuvsgul Province.

Kernel density estimation analysis

The kernel density estimation (KDE) analysis was used to identify hotspots of animal carcass disposal locations. The analysis was performed using ArcGIS v.10.6.1 software (ESRI Inc., Redlands, CA, USA) by employing the quadratic kernel function described by Silverman *et al.* (Läuter, 1988) to estimate carcass densities. The distances 88, 58, 83, and 88 km, calculated from Ripley's K function corresponding to the periods (i.e., 1986–2015, 1986–1995, 1996–2005, 2006–2015), were applied as a search radius. The KDE output is classified into five categories, according to the equal interval method.

Statistical analyses

Univariate and multivariate logistic regression models were used to determine potential risk factors associated with a large number of anthrax cases among livestock in the Khuvsgul Province. In the univariate analysis, anthrax outbreaks were categorized into a large or small number of cases. Annual cases that were above the mean of total cases (≥ 51) during the whole study period (1986–2015) were considered a large number of cases and were separately analyzed with different variables, including total livestock population, cattle population, human population, annual mean air temperature in summer months (June to August), and annual mean precipitation. In Mongolia, anthrax is a seasonal disease that mostly occurs in summer when animals graze on pastures (Odontsetseg et al., 2007). In addition, most permafrost in the Khuvsgul region is at temperatures close to 0 °C, and thaws only in summer (Sharkhuu et al., 2007), which possibly leads to spore spillover from buried carcasses to the soil surface. Thus, the effect of temperature variability in summer was investigated. The variables that met the criteria of $p < 0.2$ in the univariate analysis were further evaluated in the multivariate logistic regression model, with a statistical significance level at $p < 0.05$. Afterward, correlation tests were conducted between anthrax cases and cattle population or temperature to determine the direct relationships.

Simple linear regression analyses were used to determine livestock anthrax trends corresponding to before and after the Mongolian economic transition (1986–2000 and 2001–2015, respectively). A linear regression model was also applied to identify the annual summer (June to August) temperature changes in the Khuvsgul Province throughout the 30-year study period from 1986–2015. All statistical analyses were conducted using R v.3.5.0.

Results

Old and recent trends of anthrax between 1986 and 2015

A total of 1529 livestock cases were reported over the study period (1986–2015), with the majority of cases reported in cattle (76.5%; n = 1169), followed by horse (10.3%; n = 157), sheep (9.2%; n = 141), and goat (4.1%; n = 62) (Figures 7A and 7B). Regarding the disease prevalence in livestock by animal species for 30 years, cattle were the highest, followed by horse, sheep, and goat, with proportions of 352, 90, 12, and 4 per 100,000 population, respectively (Figure 7C). There were no anthrax reports in sheep and horses before 2000, and few outbreaks were reported in goats. After 2000, the host range expanded, and reports of anthrax incidents in goats, sheep, and other animal species had increased. Anthrax outbreaks in horses were sporadic and occurred only three times over the entire 30-year period. However, a large outbreak occurred in 2015, affecting more than 150 horses (Figure 8).

Further, simple linear regression analyses were conducted to determine livestock anthrax trends before and after the Mongolian economic transition (1986–2000 and 2001–2015, respectively). A dramatic increase was observed in the annual number of anthrax cases between 1986 and 2000, with an average rate of 10.1 ± 2.3 ($p < 0.001$) in a year. Several large outbreaks occurred after 2000, and the average annual case number was 2.5 ± 2.6 without significant increase or decrease in cases ($p = 0.35$) (Table 6). Although neither a significant increasing nor decreasing trend was observed in the total livestock anthrax cases, cattle anthrax cases were significantly reduced (Table 7).

A total of 1169 cattle anthrax cases were reported in Khuvsgul Province between 1986 and 2015. Annual cattle anthrax prevalence per 1,000,000 population per 1000 km^2 was high in the districts Murun (ID 11), Chandmani-Undur (ID 5), Khatgal (ID 24), followed by Ikh-Uul (ID 8), Tosontsengel (ID 16), and Tsagaan-Uul (ID 18) (Table 8 and Figure 9). The average human and livestock population density for 30 years was highest in the Murun district (Figure 10).

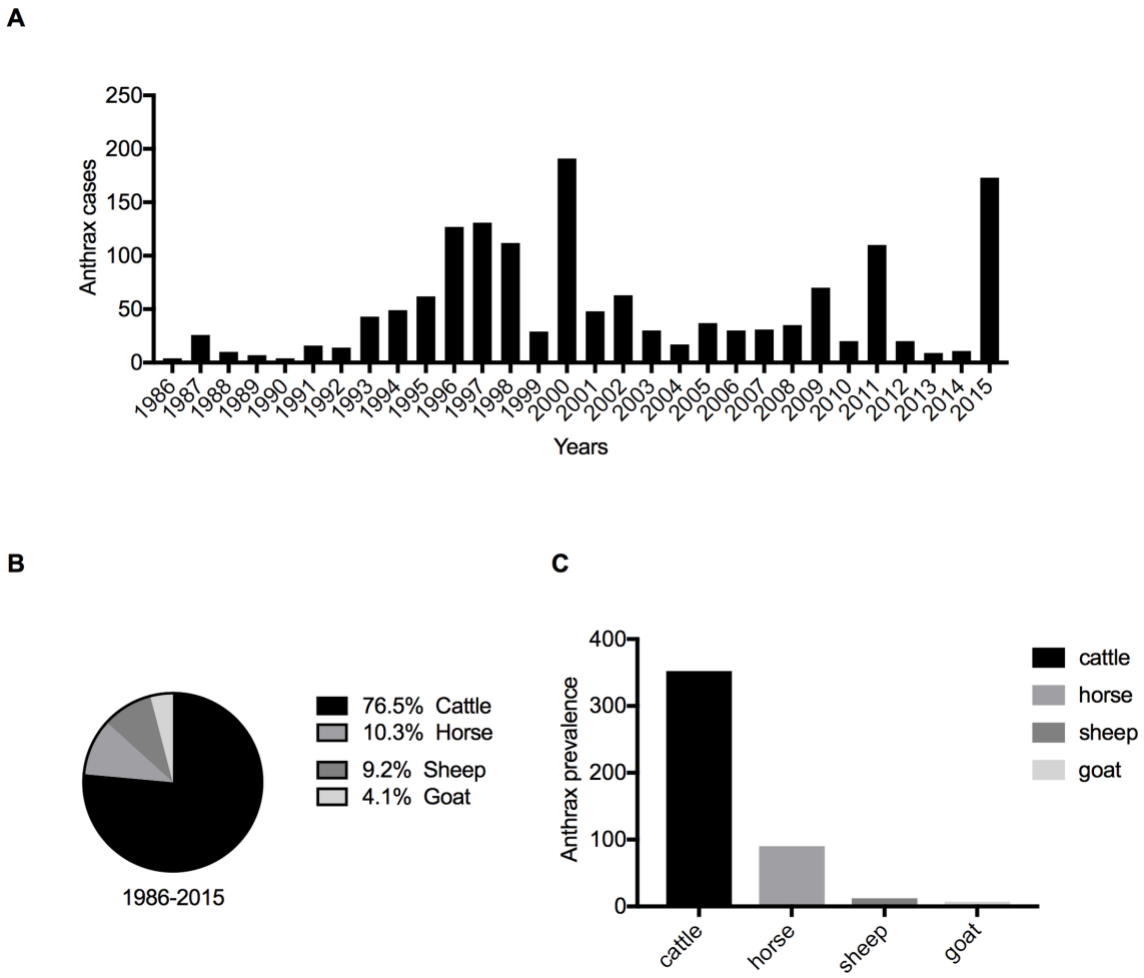

Figure 7. The distribution of anthrax in Khuvsgul Province between 1986 and 2015. (A) Annual dynamics of registered livestock anthrax cases. (B) Reported anthrax cases in livestock species. (C) Prevalence of anthrax in livestock by species for 30 years.

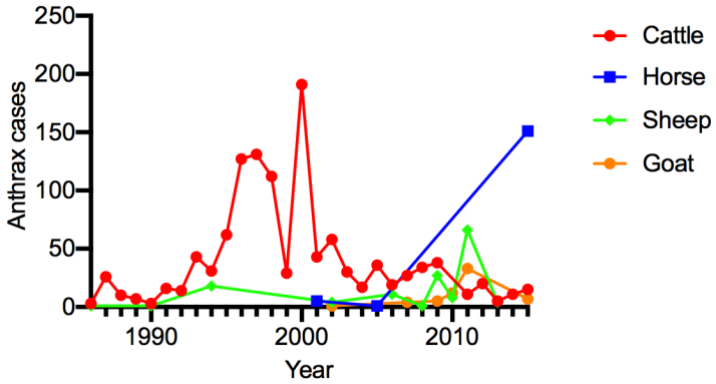

Figure 8. Anthrax in livestock species. Anthrax dynamic in livestock from 1986 to 2015.

The spatio-temporal anthrax pattern and high-risk areas

The three identified SDEs with their spatial means of carcass locations are shown in Figure 11. There were no significant directional changes in anthrax occurrence between the three periods and the spatial means of carcass sites adjoined in the southern part of the study area. By overlaying the ellipses and spatial means on an elevation map of Khuvsgul Province, it was observed that carcass sites were distributed along the rivers and seasonally dry riverbeds that confluent into wide rivers in the southern region.

To determine the distribution pattern of carcass sites and the maximum distance between carcass sites in the three periods, multi-distance spatial cluster analysis was conducted. The result indicated that the maximum distances of the significant spatial association between carcass sites corresponding to the periods (i.e., 1986–2015, 1986–1995, 1996–2005, and 2006–2015) were 88, 58, 83, and 88 km, respectively (Table 9). This result showed that carcass sites distributed in the study area are clustered rather than dispersed in the specified range of distances, and the observed relationships were statistically significant. The identified maximum distances were then used in the KDE analysis to estimate the density of carcasses to identify anthrax hotspots. consecutive anthrax hotspots were found in the southern region of the Khuvsgul Province across the entire study period and an emerging new hotspot in the northern part of the area between 2006 and 2015 (Figure 12).

Table 6. Annual livestock anthrax incidences in Khuvsgul Province during (1986–2000) and after (2001–2015) the economic transition of Mongolia.

				Linear regression		
Period	Anthrax cases in livestock	Ann[1] min	Ann[2] max	Slope	*p*	R^2
1986-2000	825	4	191	10.10 ± 2.261	0.0006	0.6058
2001-2015	704	9	173	2.529 ± 2.622	0.3524	0.06678

[1]Minimum annual number of cases; [2]Maximum annual number of cases

Table 7. Annual cattle anthrax incidences in Khuvsgul Province during (1986–2000) and after (2001–2015) the economic transition of Mongolia.

				Linear regression		
Period	Anthrax cases in cattle	Ann[1] min	Ann[2] max	Slope	*p*	R^2
1986-2000	805	3	191	10.08 ± 2.313	0.0008	0.5933
2001-2015	364	0	58	-2.475 ± 0.6898	0.0033	0.4976

[1]Minimum annual number of cases; [2]Maximum annual number of cases

964 **Table 8. Annual cattle anthrax prevalence per 1,000,000 population per 1000 km^2 in**
965 **Khuvsgul Province by districts.**

ID	District name	Number of cattle cases	Average cases (min[a]–max[b])	Average cattle population (min[c]–max[d])	Area of the districts (km^2)	Ann[1] prevalence
1	Alag-Erdene	59	1.97 (3–29)	12106 (8315–20094)	4503	36
2	Arbulag	45	1.5 (1–28)	16115 (7579–27823)	3529.2	26
3	Bayanzurkh	36	1.2 (2–20)	16275 (11593–23319)	4299.1	17
4	Burentogtokh	66	2.2 (1–26)	15174 (5755–24978)	3768.6	38
5	Chandmani-Undur	120	4 (1–42)	14054 (11159–16975)	4487.5	63
6	Erdenebulgan	34	1.13 (1–18)	13845 (10447–16497)	4694.4	17
7	Galt	32	1.07 (1–12)	17300 (9654–27537)	3596.8	17
8	Ikh-Uul	51	1.7 (1–20)	13709 (9873–18942)	2023.8	61
9	Jargalant	44	1.47 (1–15)	12624 (6100–20375)	2549.2	46
10	Khankh	16	0.53 (1–13)	8589 (903–14919)	5498.7	11
11	Murun	85	2.83 (1–24)	11200 (6207–20150)	102.9	2458
12	Rashaant	19	0.63 (1–3)	12230 (8874–17462)	1982.5	26
13	Renchinlkhumbe	121	4.03 (1–18)	22632 (16469–29020)	8448.3	21
14	Shine-Ider	25	0.83 (1–7)	13897 (7140–24723)	2053.6	29
15	Tarialan	50	1.67 (1–25)	17058 (12000–22176)	3430.7	28
16	Tosontsengel	43	1.43 (1–9)	13592 (8823–21358)	2042.2	52
17	Tsagaan-Nuur	4	0.13 (2)	2602 (835–3991)	5408.3	9
18	Tsagaan-Uul	170	5.67 (2–113)	18345 (4913–37194)	5866.3	47
19	Tsagaan-Uur	21	0.7 (2–12)	12855 (10419–15131)	8735.3	6
20	Tsetserleg	59	1.97 (1–24)	16990 (5967–33153)	7451.6	16
21	Tumurbulag	16	0.53 (1–8)	12603 (6557–19964)	2521.7	17
22	Tunel	16	0.53 (1–4)	12646 (8828–17166)	3577.3	12
23	Ulaan-Uul	27	0.9 (1–18)	18739 (13615–23438)	10057.5	5
24	Katgal	10	0.33 (4–6)	6990 (3915–9657)	911.4	52

[1]Annual anthrax prevalence per 1,000,000 cattle per 1000 km2

[a] Minimum annual number of cattle anthrax cases; [b] Maximum annual number of cattle anthrax cases

[c] The smallest annual cattle population number; [d] The largest annual cattle population number

966

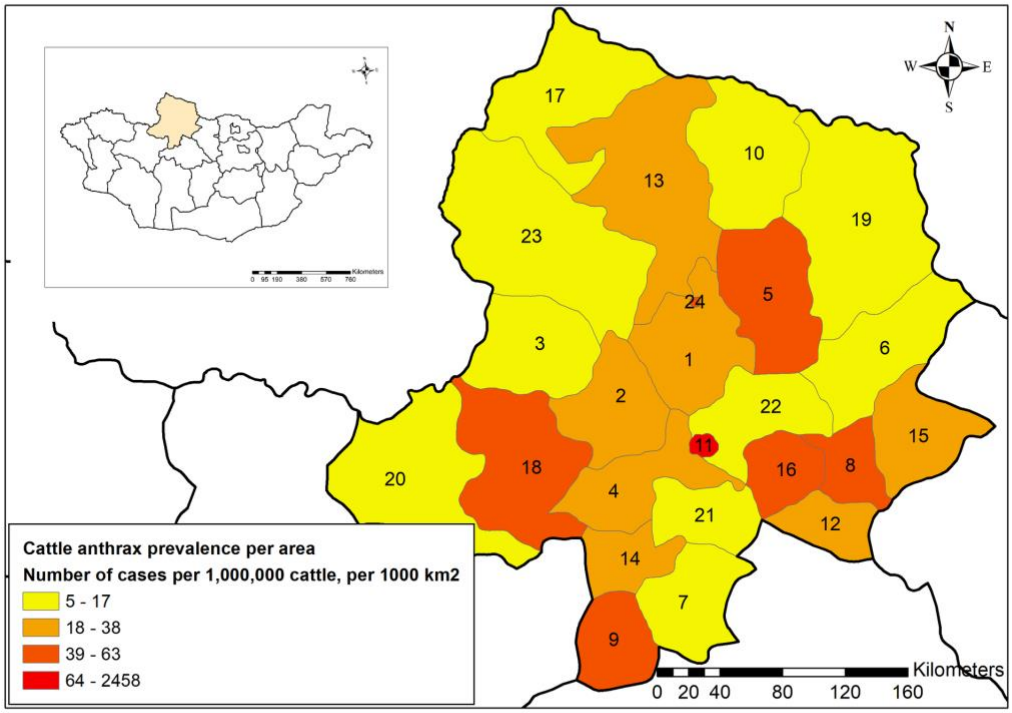

967

968 **Figure 9. Annual cattle anthrax prevalence per 1,000,000 population per 1000 km^2 in**
969 **Khuvsgul Province by districts.** Numbers correspond to the ID number in Table 8. The Murun
970 (district ID 11), the central administrative district of Khuvsgul Province, had the highest cattle
971 anthrax prevalence per area. The maps are reprinted from (Hijmans et al., 2004) under a CC
972 BY license, with permission from DIVA-GIS and Dr. Robert Hijmans.

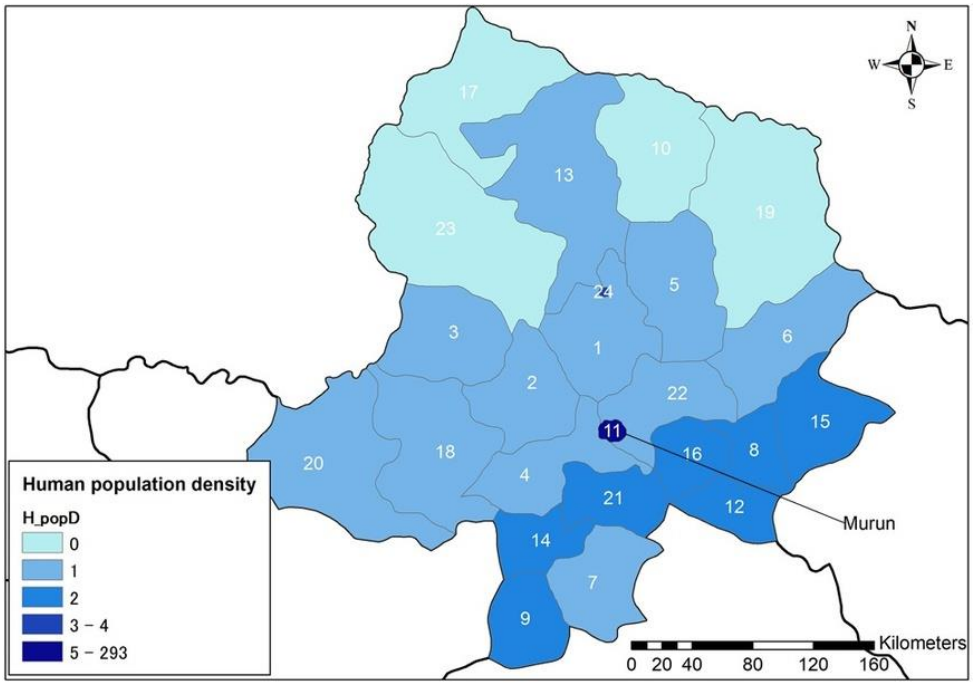

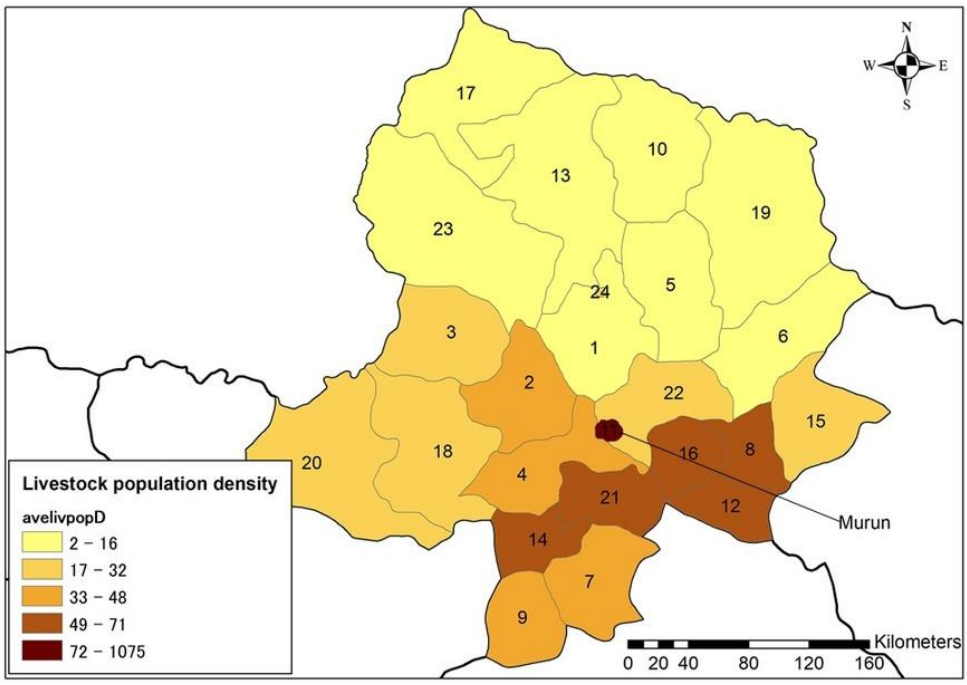

Figure 10. Average human and livestock population densities by districts of Khuvsgul Province (1986–2015). Murun district is the administrative center of the province and is estimated with the highest human and livestock population densities. The maps are reprinted from (Hijmans et al., 2004) under a CC BY license, with permission from DIVA-GIS and Dr. Robert Hijmans.

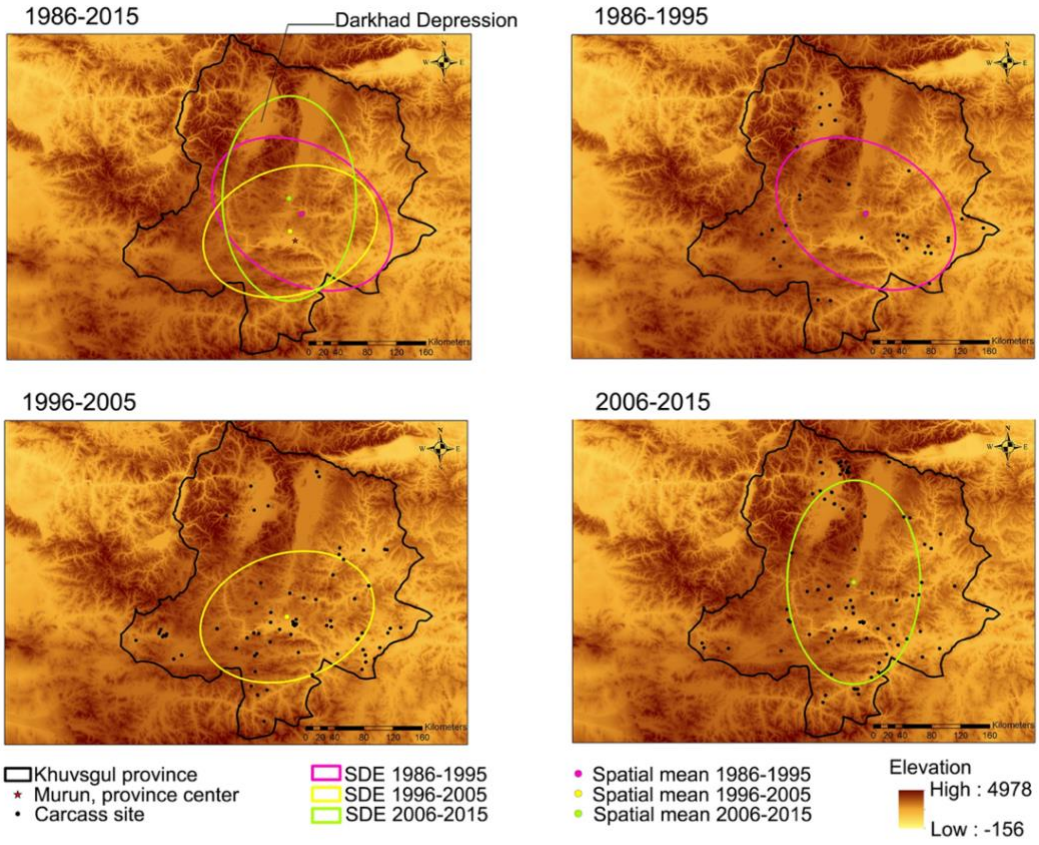

982

983 **Figure 11. The directional distribution of animal carcass sites registered between 1986**
984 **and 2015.** Unweighted spatial means and standard deviational ellipse (SDE) were determined
985 in three periods (1986–1995, 1996–2005, and 2006–2015). The unweighted spatial mean
986 centers indicate the average value of carcass locations in the given time phases. Ellipses with
987 mean centers were combined to denote the directional distribution of carcass sites. The base
988 map is the elevation in meters, with lighter areas being lower in elevation. The maps are
989 reprinted from (Hijmans et al., 2004) under a CC BY license, with permission from DIVA-GIS
990 and Dr. Robert Hijmans.

991 **Table 9. Result of multi-distance spatial cluster analyses.**

	expectedK (m)	observedK (m)	diffK (m)	LwConfEnv	HiConfEnv
1986–1995	7212.506103	17579.10497	10366.598	0	14916.3645
	14425.01221	31446.4574	17021.4452	7861.61435	24103.2532
	21637.51831	37373.68796	15736.1697	17223.9341	31837.1116
	28850.02441	44053.1086	15203.0842	22785.1231	39308.0717
	36062.53051	50092.73595	14030.2054	30244.2343	46376.8617
	43275.03662	57770.83113	14495.7945	38353.0772	54125.3735
	50487.54272	64253.97011	13766.428	45298.1825	60997.2115
	57700.04882	69698.43213	11998.3833	52029.3968	69520.8562
	64912.55492	74747.37592	9834.821	59457.9252	76464.0512
	72125.06103	8018.72247	7893.66144	66056.276	84012.6701
1996–2005	8324.025878	50481.65039	42157.6245	5820.17166	13505.5768
	16648.05176	53586.4411	36938.3893	14617.4307	22015.0963
	24972.07763	56819.80914	31847.7315	22367.3602	29456.8453
	33296.10351	60247.58951	26951.486	30712.7286	38131.2653
	41620.12939	68884.11614	27263.9867	39408.2589	45970.0043
	49944.15527	76807.26993	26863.1147	47228.1572	54954.8258
	58268.18115	83379.06679	25110.8856	55450.4559	63264.4483
	66592.20703	88679.60196	22087.3949	63715.9032	71810.3452
	74916.2329	96178.56519	21262.3323	71574.0964	79212.2517
	83240.25878	99951.69691	16711.4381	79212.2517	87719.4381
2006–2015	8813.435842	25903.4777	17090.0419	4729.30635	13652.3315
	17626.87168	35757.64284	18130.7712	13788.1789	23881.8264
	26440.30753	44364.82609	17924.5186	23408.8721	32822.431
	35253.74337	52592.49506	17338.7517	31725.1515	40911.4613
	44067.17921	62324.05206	18256.8728	41047.9091	50752.898
	52880.61505	70913.31648	18032.7014	49901.0924	59383.7187
	61694.0509	82864.14146	21170.0906	58530.142	68425.2892
	70507.48674	90538.73804	20031.2513	66182.1323	77156.8129
	79320.92258	98713.05977	19392.1372	75149.8535	85629.6171
	88134.35842	104989.8909	16855.5325	83379.8751	94487.5484
1986–2015	8821.76704	34127.46953	25305.7025	7653.6782	10929.5374
	17643.53408	39099.76416	21456.2301	16324.0946	19805.2562
	26465.30112	46413.42786	19948.1267	25122.8531	29104.9007
	35287.06816	52656.71269	17369.6445	34085.3732	37663.319
	44108.8352	61914.98147	17806.1463	42647.5556	46444.3516

	52930.60224	70904.43218	17973.8299	51067.6488	55533.7825
	61752.36928	80358.26118	18605.8919	59906.6969	64401.9258
	70574.13632	88048.28697	17474.1507	68322.2185	72936.6722
	79395.90336	95759.47909	16363.5757	76914.7807	81190.1273
	88217.6704	102592.5447	14374.8743	85190.684	89747.3321

The maximum expected K distances with statistically significant values are highlighted with gray background in the table. The spatial values corresponding to the time phases were then used for kernel density estimation analysis on anthrax carcass sites.

992

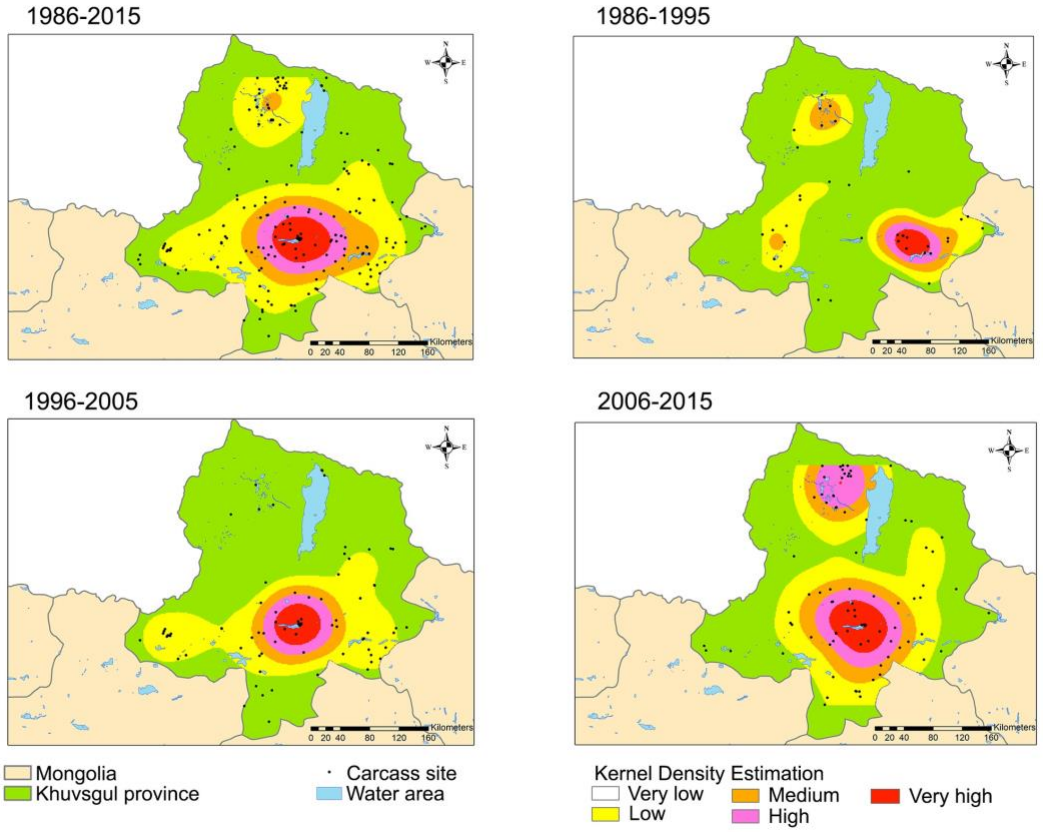

993

994 **Figure 12. Hotspot analysis of carcass sites using kernel density estimation.** The heat maps
995 show the estimated density of anthrax carcass sites per square kilometer from very low
996 (transparent) to very high (red): very low <20%, low 40%, medium 60%, high 80%, and very
997 high >80% of the estimated highest values in each period. The maps are reprinted from
998 (Hijmans et al., 2004) under a CC BY license, with permission from DIVA-GIS and Dr. Robert
999 Hijmans.

Positive association between cattle population, temperature, and anthrax case numbers

Two factors, cattle population number and annual mean temperature of summer months, have met the criteria in the initial univariate analyses. In multivariate logistic regression analysis, the odds of having a large number of anthrax cases (≥ 51) were multiplied by 7.63 for every 100,000 increase in cattle population size and by 2.86 for every 1 °C increase in mean temperature of summer (Table 10).

Cattle population, mean summer temperature, and outbreak magnitude

After identifying that cattle population and temperature are positively correlated with the anthrax case number, I investigated the extent to which the two factors affected the magnitude of an anthrax outbreak. A simple linear regression was used to model the dependence of anthrax cases on the cattle population over the entire 30-year period. A steady increase was observed in livestock population in the first half of the study period (1986–1999), followed by a decrease in 2000 before rising again in the second half (2001–2015) (Figure 13A). A drastic reduction in cattle number in 2000 was attributed to a disaster associated with severe climatic conditions, which is called zud in Mongolia. Mongolia was hit by three consecutive zuds between 1999 and 2002. Drought up to 60% of the national territory resulted in reduced pasture growth in summer and limited forage preparation by herders for the winter. Weakened by inadequate summer feeding and insufficient supplementary forage, several millions of animals died in extremely harsh winter with temperatures up to -50℃ in some areas. Overall, the national livestock population decreased by about 12 million because of the three-year sequent zud (Batima et al., 2008). A significant relationship between anthrax cases and cattle population ($r = 0.52$, $p = 0.003$) (Figure 13B) was found. The regression line's slope was 3.95 ± 1.2, suggesting that for every 10,000 increase in cattle population size, the number of anthrax cases in cattle increased by an average of about 4.

A steady rise in annual mean summer temperature of 0.08449 ± 0.02077 ($p < 0.001$) (Figure 14A) was observed, which exhibited a positive correlation with the total anthrax cases in livestock over the entire study period (1986–2015) ($r = 0.46$, $p = 0.009$) (Figure 14B). The slope of the simple linear regression line was 19.24, suggesting that for every 1 °C increase in

air temperature, the number of livestock cases increased by 19. No positive correlation was observed between the cattle population and temperature changes (Figure 15).

Table 10. Factors potentially associated with a large anthrax outbreak occurrence by univariate and multivariate logistic regression: cases (large > 51 ≥ small) *vs.* factors

Factors Univariate	OR[1]	95% CI[2] for OR[1]	$p < 0.2$
Total livestock population	1.00	1.00–1.00	0.5062
Cattle population	5.99	1.53–36.46	0.0224
Human population	1.00	1.00–1.00	0.273
Annual mean summer temperature (Jun-Aug)	2.07	1.02–5.11	0.0661
Annual mean precipitation	0.56	0.09–2.40	0.485
Year	1.04	0.95–1.15	0.3988
Factors Multivariate	**OR[1]**	**95% CI[2] for OR[1]**	**$p < 0.05$**
Cattle population	7.63	1.79–59.45	0.0172
Annual mean summer temperature (Jun-Aug)	2.86	1.16–9.71	0.0437

[1]Odds ratio; [2]Confidence interval

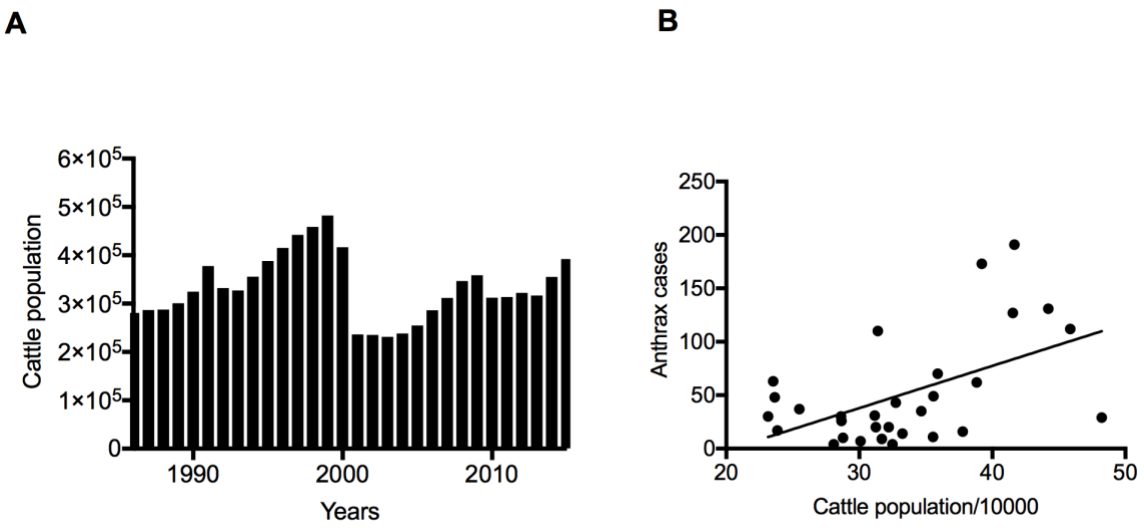

Figure 13. The magnitude of anthrax cases in relation to cattle population. (A) Cattle population by year. (B) Correlation between anthrax cases and cattle population between 1986 and 2015. r = 0.52, $p = 0.003$, 95% CI 0.2–0.743.

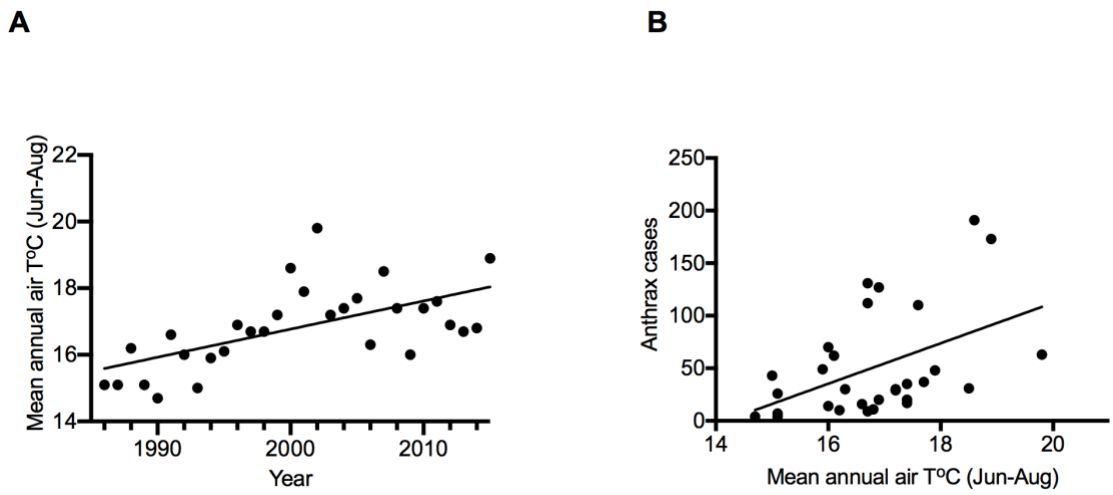

Figure 14. The magnitude of anthrax cases in relation to air temperature. (A) Linear regression of annual summer air temperature 1986–2015, slope = 0.08449 ± 0.02077, $R^2 = 0.4$, $p < 0.001$, 95% CI 0.4195–0.127. (B) Correlation between anthrax cases and annual summer air temperature from 1986 to 2015 r = 0.46, $p = 0.0099$, 95% CI 0.1238–0.7058.

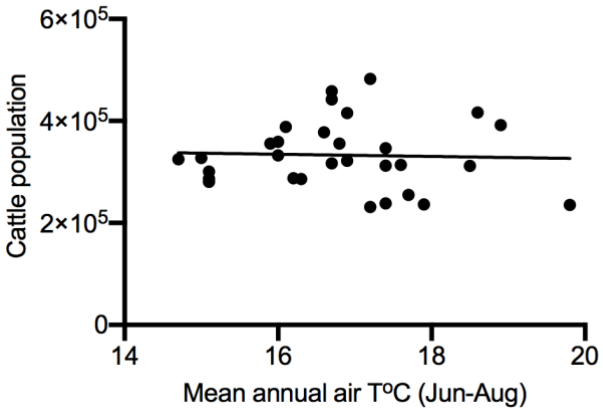

Figure 15. Interaction between temperature and cattle population. There was no correlation observed between the two risk factors with r = −0.0389, $p = 0.83$, 95% CI −0.3936–0.3259.

Discussion

Here, I report spatial and temporal patterns of anthrax in livestock between 1986 and 2015 based on the carcass burial sites of animals that died of anthrax in Khuvsgul Province, showing the highest anthrax incidence rate in Mongolia. Our primary objective was to examine the spatio-temporal dynamics of the disease based on the carcass burial sites and identify where *B. anthracis* spores may persist in the present day. First, the spatial distribution of carcass sites in three historical periods (1986–1995, 1996–2005, 2006–2015) was determined. It was found that the spatial distribution of carcass sites had not changed over the 30 years, indicating the recurrence of anthrax. Using KDE analysis on carcass sites, two hotspots were identified in low-lying areas around the south and north regions. There was a recently emerged hotspot identified in the northern part of the province in the last decade of the 30-year study period. Also, the highest proportion of anthrax cases was recorded in cattle, and cattle anthrax prevalence was high in several districts. Moreover, the disease trend during and after the transition period of the country's political change was shown. Furthermore, a positive association between outbreak size and cattle population number and the mean annual air temperature of the summer months (June to August) was observed, highlighting the impact of these factors on anthrax occurrence in Khuvsgul region.

Results of spatial mean and SDE analyses revealed a localized source of exposure of anthrax. No significant changes were observed in the distribution of anthrax carcass sites for the entire 30 years. Unweighted spatial means and spatial overlapping of three SDEs corresponding to every decade overlaid in the same geographical area. It appears that animals are repeatedly exposed to spores in the same geographical areas. This suggests that historic carcass sites are a potential hazard that serves as a source of spore exposure, resulting in recurrent outbreaks. The localized source of exposure, defined as independent outbreaks recurring in the same geographical areas, was also identified in several other spatio-temporal studies on anthrax that characterized outbreaks following a point-source pattern with limited geographical spread (Blackburn et al., 2014; Dragon et al., 2005; Driciru et al., 2018; Muturi et al., 2018). Strong, consistent spatio-temporal patterns were observed in two anthrax outbreaks in hippopotamus (*Hippopotamus amphibious*) with 5-year intervals in the same location in the Queen Elizabeth Protected Area, Uganda (Driciru et al., 2018). In addition, consecutive episodes occurred in the same area with a high density of white-tailed deer

(*Odocoileus virginianus*) carcasses in West Texas (Blackburn et al., 2014). Furthermore, concurrent and spatially localized outbreaks were observed in the Serengeti ecosystem, Tanzania (Hampson et al., 2011). Known carcass sites could likely have been the source of anthrax infection over a certain distance range (Dragon and Rennie, 1995; Dragon et al., 2001; Mongoh et al., 2008). Therefore, proper disposal of carcasses is crucial to prevent further spore exposure from affected sites.

KDE analysis identified two anthrax hotspots based on the density of animal carcasses that died of anthrax (Figure 12). One hotspot has been detected around the southern region for the entire 30 years, whereas the second hotspot emerged in the northern region in the last decade of the study period. Interestingly, both hotspots were identified in low-lying areas around the Murun district in the south and the Darkhad Depression in the north. Regarding this particular geographical feature, Van Ness previously postulated that "anthrax incubator areas" retain high spore concentrations through the water cycle in a low-lying area or depression, resulting in spore doses that are lethal to a susceptible host and enough to trigger new outbreaks (Van Ness, 1971). Supporting this postulate, carcass hotspots have been found only in low-lying areas that have wide rivers and lakes in our study (Figures 11 and 12). Notably, the Darkhad Depression encompasses many rivers, lakes, small potholes, and wetlands surrounded by mountains (Call, 2018). In agreement with our findings, Relebohile *et al*. (Lepheana et al., 2018), Bengis (Bengis, 2012), and Dragon *et al*. (Dragon and Rennie, 1995) reported a high incidence of anthrax outbreaks in depressed low-lying areas. Although the effect of water area on the number of anthrax cases was not explored in this study, I suspect that it might increase the risk of many animals being infected from one spot. Thus, the disposal of affected animal carcasses near rivers and lakes should be avoided to restrict the spore dissemination and concentration through the hydrological cycle in a low-lying area. Besides, 30-year average human and livestock population densities were highest in Murun, the administrative center of Khuvsgul Province (Figure 10). The pasture in this area could be overgrazed because of the high animal population density, thereby increasing the chance of animals ingesting or inhaling the spores. Also, anthropogenic pressure such as construction and agriculture may contribute to anthrax occurrence by exposing the spores to the ground surface, resulting in many carcass disposal sites. Therefore, human activities such as construction, mining, or agricultural development around carcass sites must be avoided, and those areas must be secured by fencing to minimize future outbreaks.

Furthermore, univariate and multivariate logistic regression analyses were conducted to determine the potential association between the number of anthrax cases in livestock and possible risk factors. I found that the population size of susceptible animals and temperature increase are the factors that impact outbreak size. Other environmental and climatic drivers, including drought, rainfall, soil alkalinity, and density of insects or scavengers, have long been recognized as important factors influencing anthrax ecology (Hugh-Jones and Blackburn, 2009). In this study, however, precipitation including rainfall, did not seem to impact the size of the outbreaks.

Cattle population number was determined as one of the risk factors for a large outbreak. From the univariate and multivariate logistic regression analyses, a significant positive correlation was found between the population number of cattle and annual anthrax cases from 1986 to 2015 (Table 10 and Figure 13B). A similar positive correlation between the number of anthrax cases and the hippopotamus population was detected in the Queen Elizabeth National Park, Uganda (Driciru et al., 2018). Hence, the susceptible animal number can be one of the determinants for outbreak size. Among the livestock species, cattle are most likely to contract anthrax in many cases (Epp et al., 2010; Mongoh et al., 2007). From the studies conducted in Kazakhstan (Aikembayev et al., 2010), China (Chen et al., 2016), and Ukraine (Bezymennyi et al., 2014), anthrax predominantly occurred in cattle compared with other animal species. In agreement with these reports, cattle anthrax occupied 76.5% of the total anthrax cases in Khuvsgul Province, and anthrax prevalence for 30 years was highest among cattle (Figures 7B and 7C), implying that cattle are the most susceptible to anthrax. Thus, in terms of resource-limited settings, cattle should be prioritized for vaccination. Moreover, cattle anthrax prevalence per 1 million population per 1000 km^2 was high in the districts Murun, Chandmani-Undur, Khatgal, followed by Ikh-Uul, Tosontsengel, and Tsagaan-Uul (Table 8 and Figure 9). Therefore, more effort in vaccination and disease surveillance should be focused on these districts with a high burden of anthrax.

Also, increased temperature was detected as another risk factor. Recent studies emphasized the impact of global warming associated with permafrost melting on anthrax occurrence in northern latitudes of the globe (Stella et al., 2020). After the reemergence of anthrax in reindeer over 70 years later in Yamal, Siberia, in 2016 (Liskova et al., 2021) and Sweden (Ågren et al., 2014), experts believed that infected animal carcasses previously buried

in these regions were long preserved under the freezing effect of permafrost. However, permafrost melting resulting from global temperature increases the spore spillovers from the carcass into the ground surface, likely through moving sediments and soil cracking related to permafrost freeze-thaw activity (Elvander et al., 2017). This hypothesis is further supported by our findings, where an increasing trend of mean annual summer temperature showed a positive correlation with the number of anthrax cases in livestock in Khuvsgul (Figures 14A and 14B). The territory of Khuvsgul comprises a wide area of mountain permafrost, which is a continuation of the southern fringe of the Siberian permafrost zone, representing the highest permafrost prevalence in Mongolia (Munkhjargal et al., 2020). From permafrost monitoring studies, the Khuvsgul region increased in mean annual permafrost temperature, coupled with intensive degradation of permafrost. These observations have been attributed to climatic factors such as global warming and anthropogenic elements like changing soil content, vegetation cover, and hydrologic cycle in the last several decades (Sharkhuu et al., 2007; Sharkhuu and Sharkhuu, 2012). To this end, the long-term anthrax persistence and the highest incidence rate in the Khuvsgul Province could be explained by the ecosystem changes, the prevalence of permafrost, and its freeze-thaw dynamics. These observations suggest that permafrost may have a role in spore persistence in soil and *B. anthracis* infection cycle, making it a potentially useful spatial and temporal predictor of infection risk and anthrax outbreaks.

I could not obtain data on the animal anthrax vaccination trends, which is a major limitation of this study. But, a previous study showed that anthrax vaccination coverage decreased between 1990 and 2000 because of the country's political revolution and economic transition phase (Odontsetseg et al., 2007). This phase involved the privatizing of animal husbandry sectors and the suspension of veterinary services, resulting in a drastic drop in the anthrax vaccination coverage and a steady increase in anthrax cases. In agreement with the study, a dramatic increase was observed in yearly livestock anthrax cases in Khuvsgul Province from 1986 to 2000 (Table 6). Similar increasing anthrax trends were seen in other former Soviet countries, which was likely a result of socio-political instability (Bezymennyi et al., 2014; Kracalik et al., 2014). Taken together, these findings highlight that Mongolia's political change and economic transition affected anthrax occurrence, more likely through livestock vaccination. Since 2000, although neither a significant increasing nor decreasing trend was observed in the total livestock anthrax cases, cattle anthrax cases were significantly reduced, which had progressively increased during the transition period (Table 7). It can be speculated that the

1174 downslope in cattle anthrax cases was likely associated with improving disease control
1175 measures, particularly cattle vaccination (Odontsetseg et al., 2007). Further, extending
1176 vaccination to livestock species excluded in routine vaccination programs is on demand for
1177 successful disease control in Mongolia, especially in areas with high-risk factors.

General conclusion

The long-time persistence of highly resistant anthrax spores in the environment and its detrimental risk to animal and human health have been a great concern. Anthrax continues to pose a serious public health and socioeconomic threat in several developing countries, and it tends to re-emerge in some places after a long period of absence. Based on various recently published literatures, the geographic distribution of anthrax is predicted to expand with continued warming, suggesting that countries need to strengthen outbreak preparedness and develop practical control strategies. However, the lack of detailed serological and epidemiological data in many developing countries limits the successful implementation of effective anthrax control policies. Presently, there is a lack of serological assays and epidemiological information to develop an anthrax management and control strategy in many countries, including Mongolia. Therefore, this work provides a serological tool that can be utilized to improve anthrax serosurveillance worldwide. Furthermore, using Mongolia's Khuvsgul Province as an example, the project demonstrates how GIS data on carcass sites can be valuable for predicting anthrax hotspots that may serve as infection sources for future outbreaks.

In chapter I, a new ELISA test to detecting naturally acquired antibodies against anthrax infection was developed. This ELISA was established based on *B. anthracis* pXO2 plasmid, which lacks in animal vaccine strains, thus distinguishing them from virulent strains. This research has demonstrated two immunoreactive antigens encoded on the pXO2 plasmid; the capsule biosynthesis protein CapA and peptide ABC transporter substrate-binding protein. Concerning the antigen specificity, immunoreactivity, and solubility of protein expression, the C-terminus end of capsule biosynthesis protein CapA, named CapA322, was further selected and used for CapA322-ELISA development. The CapA322-ELISA was shown to be specific and non-cross-reactive to sera from horses vaccinated with *B. anthracis* Sterne 34F2 strain live spore vaccine. Hence, the CapA322-ELISA can be used to detect naturally acquired antibodies and ascertain the immunological state of animals. While the results presented here are satisfactory, further research is essential to optimize the CapA322-ELISA. Such future work will involve field studies of livestock in endemic and non-endemic areas to validate the assay.

In chapter II, spatial and temporal patterns of anthrax carcass sites in Khuvsgul Province, Mongolia were analyzed to inform the geographical distribution and hotspot areas of carcass sites as they are potential infection sources. Moreover, 30-year retrospective data (1986–2015) of anthrax cases among livestock in Khuvsgul Province was analyzed to reveal past and recent trends of the disease, anthrax prevalence in districts, and its burden in animals. Furthermore, the study investigated the risk factors that possibly influence anthrax occurrence to understand hyperendemicity of anthrax in this province.

The results showed that the spatial distribution of carcass sites had not changed over the 30 years, indicating the recurrence of anthrax. There was one stable hotspot of anthrax carcass sites around the south and an emerging new one in the north region of the province. These hotspots exist in low-lying areas with abundant rivers, lakes, and ponds. Further, the burden of anthrax was higher in cattle than in other livestock species, and the cattle anthrax prevalence was high in the six districts. Finally, the size of outbreaks was influenced by the annual summer mean air temperature (June to August) of Khuvsgul Province, probably by affecting the permafrost freeze-thawing activity.

The study suggests that historical carcass burial sites may serve as a persistent source of anthrax infection. Thus, regarding the primary action for carcass disposal management, it can be recommended that fencing the old carcass sites to prevent possible animal spore exposure. Further, burying animal carcasses that died of anthrax should be banned and replaced by incineration, considering long-time preservation of *B. anthracis* spores in the frozen ground (permafrost) and its seasonal thawing effect on spore spillover to the soil surface. At least carcass disposal near rivers and lakes should be avoided to minimize spore dissemination and concentration through the hydrological cycle. As additional anthrax control measures, this study recommends the strategic vaccination of susceptible animals, especially prioritizing cattle in the six districts mentioned above. Another suggestion would be monitoring the permafrost condition in endemic areas, which could be helpful to predict future outbreaks and design epidemic preparedness plans. Future work should involve detailed field surveys on spore viability around the carcass burial sites and molecular epidemiology of the *B. anthracis* strains.

Overall, the work presented here highlights a new approach for investigating anthrax. Firstly, it introduces a novel diagnostic tool that can be used to collect surveillance data

prospectively. Secondly, using data from Mongolia, the study emphasizes the importance of retrospective data in identifying high risk areas to prevent future outbreaks.

Acknowledgments

It is my greatest pleasure to express my sincerest gratitude to Professor Hideaki Higashi, my principal supervisor and head of the Division of Infection and Immunity, International Institute for Zoonosis Control, Hokkaido University, for giving me an opportunity to study in the doctoral course in Japan and for the advice and continuous support he provided throughout my studies as his student. I have been lucky enough to work under the leadership of a supervisor who cares so much about my academic progress.

I am deeply grateful to Senior Assistant Professor Yoshikazu Furuta at the Division of Infection and Immunity, International Institute for Zoonosis Control, Hokkaido University, for closely supervising me and teaching me about having the correct scientific approach. I especially appreciate your persistent support, which was influential in shaping my experiment methods and critiquing skills. Your consistency, immense knowledge, and abundant experience have inspired me in all the time of my academic research.

I am grateful to Assistant Professor Atmika Paudel at the Division of Infection and Immunity, International Institute for Zoonosis Control, Hokkaido University, for her guidance and suggestions on my study and career path during and after graduation from my Ph.D. course.

I would also like to thank Dr. Jargalsaikhan Enkhtuya and members of the anthrax team at the Institute of Veterinary Medicine, Mongolia, Dr. Nasalmaa Myagmar at State Central Veterinary Laboratory, Mongolia, and everyone working at the Department of Veterinary Services of Khuvsgul Province, Mongolia, for their valuable cooperation and contribution in my Ph.D. research studies.

Many thanks to Dr. Manyando Simbotwe at the Division of Infection and Immunity, International Institute for Zoonosis Control, Hokkaido University, for the technical support and guidance.

Special thanks to Dr. Akihiro Ochi at Equine Research Institute, Japan Racing Association, Tochigi, Japan, for providing vaccinated horse serum samples.

My gratitude extends to Dr. Norikazu Isoda at the Laboratory of Microbiology, School of Veterinary Medicine, Hokkaido University and Dr. Satoshi Ito at Unit of Risk Analysis and Management, International Institute for Zoonosis Control, Hokkaido University for their tremendous help and guidance on the implementation and interpretation of the fundamental principles of the spatio-temporal epidemiology of infectious diseases.

I appreciate the Department of Veterinary Services of Khuvsgul Province, Mongolia for cooperation in epidemiological data provision for livestock anthrax outbreaks. My sincerest thanks to Dr. Enkhbat Erdenebat for assistance with meteorological data collection.

I would like to acknowledge the professional support of Professor Yasuhiko Suzuki at the Division of Bioresources, and Associate professor Junya Yamagishi at the Division of Collaboration and Education, International Institute for Zoonosis Control Hokkaido University.

I would also like to thank all my friends, colleagues, lab mates, and collaborators who I've ever worked with at the Division of Infection and Immunity, International Institute Center for Zoonosis Control, for making my stay in Japan memorable. Dr. Misheck Shawa, my dearest friend and lab colleague, I owe a special thank you for always cheering me on since the very first day at school and lab.

Finally, I would like to express my gratitude to my family. Without their enormous understanding and encouragement in the past few years, it would be impossible for me to complete my study.

Reference

Aikembayev, A. M., L. Lukhnova, G. Temiraliyeva, T. Meka-Mechenko, Y. Pazylov, S. Zakaryan, G. Denissov, W. R. Easterday, M. N. Van Ert, P. Keim, S. C. Francesconi, J. K. Blackburn, M. Hugh-Jones, and T. Hadfield, 2010, Historical distribution and molecular diversity of Bacillus anthracis, Kazakhstan: Emerg Infect Dis, v. 16, p. 789-796.

Ariel, N., A. Zvi, H. Grosfeld, O. Gat, Y. Inbar, B. Velan, S. Cohen, and A. Shafferman, 2002, Search for potential vaccine candidate open reading frames in the Bacillus anthracis virulence plasmid pXO1: in silico and in vitro screening: Infect Immun, v. 70, p. 6817-6827.

Badmaeva, O. B., B. Bayanzhargal, and V. C. Tsydypov, 2014, The epizootiological indicators of anthrax in Mongolia: Vestnik OrelGAU, v. 46, p. 14-16.

Baldwin, V. M., 2020, You Can't B. cereus – A Review of Bacillus cereus Strains That Cause Anthrax-Like Disease: Frontiers in Microbiology, v. 11, p. 1731.

Batima, P., L. Natsagdorj, and N. Batnasan, 2008, Vulnerability of Mongolia's pastoralists to climate extremes and changes: Climate change and vulnerability, v. 2, p. 67-87.

Ben-Noun, L., 2002, [Characteristics of anthrax: its description and biblical name--Shehin]: Harefuah, v. 141 Spec No, p. 4-6, 124.

Bengis, R. G., 2012, Chapter 13 - Anthrax in Free-Ranging Wildlife, *in* R. E. Miller, and M. Fowler, eds., Fowler's Zoo and Wild Animal Medicine: Saint Louis, W.B. Saunders, p. 98-107.

Beradze, I., 2019, Anthrax Laboratory Diagnostic Methods at the Laboratory of the Ministry of Agriculture (LMA), Online J Public Health Inform, v. 11, ISDS Annual Conference Proceedings 2019.

Beyer, W., P. Glöckner, J. Otto, and R. Böhm, 1995, A nested PCR method for the detection of Bacillus anthracis in environmental samples collected from former tannery sites: Microbiological Research, v. 150, p. 179-186.

1312 Beyer, W., and P. C. Turnbull, 2009, Anthrax in animals: Mol Aspects Med, v. 30, p. 481-489.

1313 Bezymennyi, M., K. H. Bagamian, A. Barro, A. Skrypnyk, V. Skrypnyk, and J. K. Blackburn,
1314 2014, Spatio-temporal patterns of livestock anthrax in Ukraine during the past century
1315 (1913–2012): Applied Geography, v. 54, p. 129-138.

1316 Blackburn, J. K., T. L. Hadfield, A. J. Curtis, and M. E. Hugh-Jones, 2014, Spatial and
1317 Temporal Patterns of Anthrax in White-Tailed Deer, Odocoileus virginianus, and
1318 Hematophagous Flies in West Texas during the Summertime Anthrax Risk Period:
1319 Annals of the Association of American Geographers, v. 104, p. 939-958.

1320 Cachat, E., M. Barker, T. D. Read, and F. G. Priest, 2008, A Bacillus thuringiensis strain
1321 producing a polyglutamate capsule resembling that of Bacillus anthracis: FEMS
1322 Microbiol Lett, v. 285, p. 220-226.

1323 Call, M., 2018, A Waterbird Inventory of the Darkhad Depression, Kbovsgol, Mongolia.

1324 Candela, T., and A. Fouet, 2005, Bacillus anthracis CapD, belonging to the gamma-
1325 glutamyltranspeptidase family, is required for the covalent anchoring of capsule to
1326 peptidoglycan: Mol Microbiol, v. 57, p. 717-726.

1327 Carlson, C. J., W. M. Getz, K. L. Kausrud, C. A. Cizauskas, J. K. Blackburn, F. A. Bustos
1328 Carrillo, R. Colwell, W. R. Easterday, H. H. Ganz, P. L. Kamath, O. A. Økstad, W. C.
1329 Turner, A. B. Kolstø, and N. C. Stenseth, 2018, Spores and soil from six sides:
1330 interdisciplinarity and the environmental biology of anthrax (Bacillus anthracis): Biol
1331 Rev Camb Philos Soc, v. 93, p. 1813-1831.

1332 Carlson, C. J., I. T. Kracalik, N. Ross, K. A. Alexander, M. E. Hugh-Jones, M. Fegan, B. T.
1333 Elkin, T. Epp, T. K. Shury, W. Zhang, M. Bagirova, W. M. Getz, and J. K. Blackburn,
1334 2019, The global distribution of Bacillus anthracis and associated anthrax risk to
1335 humans, livestock and wildlife: Nature Microbiology, v. 4, p. 1337-1343.

1336 Chakravarti, D. N., M. J. Fiske, L. D. Fletcher, and R. J. Zagursky, 2000, Application of
1337 genomics and proteomics for identification of bacterial gene products as potential
1338 vaccine candidates: Vaccine, v. 19, p. 601-612.

Chaudhuri, R., D. Kulshreshtha, M. V. Raghunandanan, and S. Ramachandran, 2014, Integrative immunoinformatics for Mycobacterial diseases in R platform: Syst Synth Biol, v. 8, p. 27-39.

Chen, W. J., S. J. Lai, Y. Yang, K. Liu, X. L. Li, H. W. Yao, Y. Li, H. Zhou, L. P. Wang, D. Mu, W. W. Yin, L. Q. Fang, H. J. Yu, and W. C. Cao, 2016, Mapping the Distribution of Anthrax in Mainland China, 2005-2013: PLoS Negl Trop Dis, v. 10, p. e0004637.

Chen, Z., R. Schneerson, J. A. Lovchik, Z. Dai, J. Kubler-Kielb, L. Agulto, S. H. Leppla, and R. H. Purcell, 2015, Bacillus anthracis Capsular Conjugates Elicit Chimpanzee Polyclonal Antibodies That Protect Mice from Pulmonary Anthrax: Clin Vaccine Immunol, v. 22, p. 902-908.

Chitlaru, T., O. Gat, H. Grosfeld, I. Inbar, Y. Gozlan, and A. Shafferman, 2007, Identification of In Vivo-Expressed Immunogenic Proteins by Serological Proteome Analysis of the Bacillus anthracis Secretome: Infection and Immunity, v. 75, p. 2841-2852.

Cieslak, T. J., and E. M. Eitzen, Jr., 1999, Clinical and epidemiologic principles of anthrax: Emerg Infect Dis, v. 5, p. 552-555.

Crowther, J. R., 2000, The ELISA guidebook: Methods Mol Biol, v. 149, 1-413 p.

Dragon, D. C., D. E. Bader, J. Mitchell, and N. Woollen, 2005, Natural dissemination of *Bacillus anthracis* spores in northern Canada: Appl Environ Microbiol, v. 71, p. 1610-1615.

Dragon, D. C., and R. P. Rennie, 1995, The ecology of anthrax spores: tough but not invincible: Can Vet J, v. 36, p. 295-301.

Dragon, D. C., R. P. Rennie, and B. T. Elkin, 2001, Detection of anthrax spores in endemic regions of northern Canada: J Appl Microbiol, v. 91, p. 435-441.

Driciru, M., I. B. Rwego, B. Asiimwe, D. A. Travis, J. Alvarez, K. VanderWaal, and K. Pelican, 2018, Spatio-temporal epidemiology of anthrax in Hippopotamus amphibious in Queen Elizabeth Protected Area, Uganda: PLoS One, v. 13, p. e0206922.

1365 Drysdale, M., S. Heninger, J. Hutt, Y. Chen, C. R. Lyons, and T. M. Koehler, 2005, Capsule
1366 synthesis by Bacillus anthracis is required for dissemination in murine inhalation
1367 anthrax: Embo j, v. 24, p. 221-227.

1368 Duesbery, N. S., C. P. Webb, S. H. Leppla, V. M. Gordon, K. R. Klimpel, T. D. Copeland, N.
1369 G. Ahn, M. K. Oskarsson, K. Fukasawa, K. D. Paull, and G. F. Vande Woude, 1998,
1370 Proteolytic inactivation of MAP-kinase-kinase by anthrax lethal factor: Science, v. 280,
1371 p. 734-737.

1372 Ebright, J. R., T. Altantsetseg, and R. Oyungerel, 2003, Emerging infectious diseases in
1373 Mongolia: Emerg Infect Dis, v. 9, p. 1509-1515.

1374 Elvander, M., B. Persson, and S. Sternberg Lewerin, 2017, Historical cases of anthrax in
1375 Sweden 1916-1961, v. 64, p. 892-898.

1376 Emanuelsson, O., S. Brunak, G. von Heijne, and H. Nielsen, 2007, Locating proteins in the cell
1377 using TargetP, SignalP and related tools: Nat Protoc, v. 2, p. 953-971.

1378 Environmental Systems Research Institute, Directional Distribution (Standard Deviational
1379 Ellipse).

1380 Environmental Systems Research Institute, Multi-Distance Spatial Cluster Analysis (Ripley's
1381 K Function).

1382 Epp, T., C. Waldner, and C. K. Argue, 2010, Case-control study investigating an anthrax
1383 outbreak in Saskatchewan, Canada--Summer 2006: Can Vet J, v. 51, p. 973-978.

1384 Fasanella, A., D. Galante, G. Garofolo, and M. H. Jones, 2010, Anthrax undervalued zoonosis:
1385 Vet Microbiol, v. 140, p. 318-331.

1386 Fox, M. D., J. M. Boyce, A. F. Kaufmann, J. B. Young, and H. W. Whitford, 1977, An
1387 epizootiologic study of anthrax in Falls County, Texas: J Am Vet Med Assoc, v. 170,
1388 p. 327-333.

1389 Ganeva.D.J., 2004, Analysis of the bulgarian tabanid fauna with regard to its potential for
1390 epidemiological involvement: Bulgarian Journal of Veterinary Medicine, v. 7, p. 1-8.

Gat, O., H. Grosfeld, N. Ariel, I. Inbar, G. Zaide, Y. Broder, A. Zvi, T. Chitlaru, Z. Altboum, D. Stein, S. Cohen, and A. Shafferman, 2006, Search for Bacillus anthracis potential vaccine candidates by a functional genomic-serologic screen: Infect Immun, v. 74, p. 3987-4001.

General Authority for Veterinary Services, 2019, Standard Operating Procedure for Prevention and Control Anthrax in Animal.

Ghosh, N., and A. K. Goel, 2012, Anti-Protective Antigen IgG Enzyme-Linked Immunosorbent Assay for Diagnosis of Cutaneous Anthrax in India: Clinical and Vaccine Immunology, v. 19, p. 1238-1242.

Ghosh, N., I. Tomar, H. Lukka, and A. K. Goel, 2013, Serodiagnosis of Human Cutaneous Anthrax in India Using an Indirect Anti-Lethal Factor IgG Enzyme-Linked Immunosorbent Assay: Clinical and Vaccine Immunology, v. 20, p. 282-286.

Gibson, D. G., L. Young, R. Y. Chuang, J. C. Venter, C. A. Hutchison, 3rd, and H. O. Smith, 2009, Enzymatic assembly of DNA molecules up to several hundred kilobases: Nat Methods, v. 6, p. 343-345.

Glinert, I., S. Weiss, A. Sittner, E. Bar-David, A. Ben-Shmuel, J. Schlomovitz, D. Kobiler, and H. Levy, 2018, Infection with a Nonencapsulated Bacillus anthracis Strain in Rabbits-The Role of Bacterial Adhesion and the Potential for a Safe Live Attenuated Vaccine: Toxins (Basel), v. 10, p. 506.

Grabenstein, J. D., 2008, Vaccines: countering anthrax: vaccines and immunoglobulins: Clin Infect Dis, v. 46, p. 129-136.

Hampson, K., T. Lembo, P. Bessell, H. Auty, C. Packer, J. Halliday, C. A. Beesley, R. Fyumagwa, R. Hoare, E. Ernest, C. Mentzel, K. L. Metzger, T. Mlengeya, K. Stamey, K. Roberts, P. P. Wilkins, and S. Cleaveland, 2011, Predictability of anthrax infection in the Serengeti, Tanzania: J Appl Ecol, v. 48, p. 1333-1344.

Han, C. S., G. Xie, J. F. Challacombe, M. R. Altherr, S. S. Bhotika, N. Brown, D. Bruce, C. S. Campbell, M. L. Campbell, J. Chen, O. Chertkov, C. Cleland, M. Dimitrijevic, N. A. Doggett, J. J. Fawcett, T. Glavina, L. A. Goodwin, L. D. Green, K. K. Hill, P. Hitchcock,

P. J. Jackson, P. Keim, A. R. Kewalramani, J. Longmire, S. Lucas, S. Malfatti, K. McMurry, L. J. Meincke, M. Misra, B. L. Moseman, M. Mundt, A. C. Munk, R. T. Okinaka, B. Parson-Quintana, L. P. Reilly, P. Richardson, D. L. Robinson, E. Rubin, E. Saunders, R. Tapia, J. G. Tesmer, N. Thayer, L. S. Thompson, H. Tice, L. O. Ticknor, P. L. Wills, T. S. Brettin, and P. Gilna, 2006, Pathogenomic sequence analysis of Bacillus cereus and Bacillus thuringiensis isolates closely related to Bacillus anthracis: J Bacteriol, v. 188, p. 3382-3390.

Harrison, L. H., J. W. Ezzell, T. G. Abshire, S. Kidd, and A. F. Kaufmann, 1989, Evaluation of serologic tests for diagnosis of anthrax after an outbreak of cutaneous anthrax in Paraguay: J Infect Dis, v. 160, p. 706-710.

Hijmans, R. J., L. Guarino, C. Bussink, P. Mathur, M. Cruz, I. Barrentes, and E. Rojas, 2004, DIVA-GIS.

Hoffmaster, A. R., K. K. Hill, J. E. Gee, C. K. Marston, B. K. De, T. Popovic, D. Sue, P. P. Wilkins, S. B. Avashia, R. Drumgoole, C. H. Helma, L. O. Ticknor, R. T. Okinaka, and P. J. Jackson, 2006, Characterization of Bacillus cereus isolates associated with fatal pneumonias: strains are closely related to Bacillus anthracis and harbor B. anthracis virulence genes: J Clin Microbiol, v. 44, p. 3352-3360.

Hugh-Jones, M., and J. Blackburn, 2009, The ecology of Bacillus anthracis: Molecular aspects of medicine, v. 30, p. 356-367.

Hugh-Jones, M. E., and V. de Vos, 2002, Anthrax and wildlife: Rev Sci Tech, v. 21, p. 359-383.

Hulo, N., A. Bairoch, V. Bulliard, L. Cerutti, B. A. Cuche, E. de Castro, C. Lachaize, P. S. Langendijk-Genevaux, and C. J. Sigrist, 2008, The 20 years of PROSITE: Nucleic Acids Res, v. 36, p. 245-249.

Ivins, B., P. Fellows, L. Pitt, J. Estep, J. Farchaus, A. Friedlander, and P. Gibbs, 1995, Experimental anthrax vaccines: efficacy of adjuvants combined with protective antigen against an aerosol Bacillus anthracis spore challenge in guinea pigs: Vaccine, v. 13, p. 1779-1784.

Ivins, B. E., M. L. Pitt, P. F. Fellows, J. W. Farchaus, G. E. Benner, D. M. Waag, S. F. Little, G. W. Anderson, Jr., P. H. Gibbs, and A. M. Friedlander, 1998, Comparative efficacy of experimental anthrax vaccine candidates against inhalation anthrax in rhesus macaques: Vaccine, v. 16, p. 1141-1148.

Ivins, B. E., S. L. Welkos, S. F. Little, M. H. Crumrine, and G. O. Nelson, 1992, Immunization against anthrax with Bacillus anthracis protective antigen combined with adjuvants: Infect Immun, v. 60, p. 662-668.

Jefferson, T., M. Rudin, and C. DiPietrantonj, 2003, Systematic review of the effects of pertussis vaccines in children: Vaccine, v. 21, p. 2003-2014.

Jelacic, T. M., D. J. Chabot, J. A. Bozue, S. A. Tobery, M. W. West, K. Moody, D. Yang, J. J. Oppenheim, and A. M. Friedlander, 2014, Exposure to Bacillus anthracis capsule results in suppression of human monocyte-derived dendritic cells: Infect Immun, v. 82, p. 3405-3416.

Jeong, H., H. J. Kim, and S. J. Lee, 2015, Complete Genome Sequence of Escherichia coli Strain BL21: Genome Announc, v. 3, p. e00134-15.

Juncker, A. S., H. Willenbrock, G. Von Heijne, S. Brunak, H. Nielsen, and A. Krogh, 2003, Prediction of lipoprotein signal peptides in Gram-negative bacteria: Protein Sci, v. 12, p. 1652-1662.

Kanankege, K. S. T., S. K. Abdrakhmanov, J. Alvarez, L. Glaser, J. B. Bender, Y. Y. Mukhanbetkaliyev, F. I. Korennoy, A. S. Kadyrov, A. S. Abdrakhmanova, and A. M. Perez, 2019, Comparison of spatiotemporal patterns of historic natural Anthrax outbreaks in Minnesota and Kazakhstan: PLoS One, v. 14, p. e0217144.

Kaufmann, A. F., and A. L. Dannenberg, 2002, Age as a risk factor for cutaneous human anthrax: evidence from Haiti, 1973-1974, Emerg Infect Dis, v. 8, p. 874-875.

Kempsell, K. E., S. P. Kidd, K. Lewandowski, M. J. Elmore, S. Charlton, A. Yeates, H. Cuthbertson, B. Hallis, D. M. Altmann, M. Rogers, P. Wattiau, R. J. Ingram, T. Brooks, and R. Vipond, 2015, Whole genome protein microarrays for serum profiling of immunodominant antigens of Bacillus anthracis: Front Microbiol, v. 6, p. 747.

Kim, K., J. Seo, K. Wheeler, C. Park, D. Kim, S. Park, W. Kim, S. I. Chung, and T. Leighton, 2005, Rapid genotypic detection of Bacillus anthracis and the Bacillus cereus group by multiplex real-time PCR melting curve analysis: FEMS Immunol Med Microbiol, v. 43, p. 301-310.

Klee, S. R., E. B. Brzuszkiewicz, H. Nattermann, H. Brüggemann, S. Dupke, A. Wollherr, T. Franz, G. Pauli, B. Appel, W. Liebl, E. Couacy-Hymann, C. Boesch, F. D. Meyer, F. H. Leendertz, H. Ellerbrok, G. Gottschalk, R. Grunow, and H. Liesegang, 2010, The genome of a Bacillus isolate causing anthrax in chimpanzees combines chromosomal properties of B. cereus with B. anthracis virulence plasmids: PLoS One, v. 5, p. e10986.

Koch, R., 1876, Die Ätiologie der Milzbrand-Krankheit, begründet auf die Entwicklungsgeschichte des Bacillus Anthracis, Robert Koch-Institut.

Kracalik, I., R. Abdullayev, K. Asadov, R. Ismayilova, M. Baghirova, N. Ustun, M. Shikhiyev, A. Talibzade, and J. K. Blackburn, 2014, Changing patterns of human anthrax in Azerbaijan during the post-Soviet and preemptive livestock vaccination eras: PLoS Negl Trop Dis, v. 8, p. e2985.

Krogh, A., B. Larsson, G. von Heijne, and E. L. Sonnhammer, 2001, Predicting transmembrane protein topology with a hidden Markov model: application to complete genomes: J Mol Biol, v. 305, p. 567-580.

Lembo, T., K. Hampson, H. Auty, C. A. Beesley, P. Bessell, C. Packer, J. Halliday, R. Fyumagwa, R. Hoare, E. Ernest, C. Mentzel, T. Mlengeya, K. Stamey, P. P. Wilkins, and S. Cleaveland, 2011, Serologic surveillance of anthrax in the Serengeti ecosystem, Tanzania, 1996-2009: Emerg Infect Dis, v. 17, p. 387-394.

Lepheana, R. J., J. W. Oguttu, and D. N. Qekwana, 2018, Temporal patterns of anthrax outbreaks among livestock in Lesotho, 2005-2016: PLoS One, v. 13, p. e0204758.

Leppla, S. H., 1982, Anthrax toxin edema factor: a bacterial adenylate cyclase that increases cyclic AMP concentrations of eukaryotic cells: Proc Natl Acad Sci U S A, v. 79, p. 3162-3166.

Liskova, E. A., I. Y. Egorova, Y. O. Selyaninov, I. V. Razheva, N. A. Gladkova, N. N. Toropova, O. I. Zakharova, O. A. Burova, G. V. Surkova, S. M. Malkhazova, F. I. Korennoy, I. V. Iashin, and A. A. Blokhin, 2021, Reindeer Anthrax in the Russian Arctic, 2016: Climatic Determinants of the Outbreak and Vaccination Effectiveness: Frontiers in Veterinary Science, v. 8, p. 486.

Lu, S., J. Wang, F. Chitsaz, M. K. Derbyshire, R. C. Geer, N. R. Gonzales, M. Gwadz, D. I. Hurwitz, G. H. Marchler, J. S. Song, N. Thanki, R. A. Yamashita, M. Yang, D. Zhang, C. Zheng, C. J. Lanczycki, and A. Marchler-Bauer, 2020, CDD/SPARCLE: the conserved domain database in 2020: Nucleic Acids Res, v. 48, p. 265-268.

Läuter, H., 1988, Silverman, BW: Density Estimation for Statistics and Data Analysis: Biometrical Journal, v. 30, p. 876-877.

Marcus, H., R. Danieli, E. Epstein, B. Velan, A. Shafferman, and S. Reuveny, 2004, Contribution of immunological memory to protective immunity conferred by a Bacillus anthracis protective antigen-based vaccine: Infect Immun, v. 72, p. 3471-3477.

María, R. A., J. Castelán, J. Alicia, G. Monterrubio, and A. Gerardo, 2017, The Impact of Bioinformatics on Vaccine Design and Development.

McWilliams, B. D., T. Palzkill, G. M. Weinstock, and J. F. Petrosino, 2012, Identification of novel and cross-species seroreactive proteins from Bacillus anthracis using a ligation-independent cloning-based, SOS-inducible expression system: Microbial Pathogenesis, v. 53, p. 250-258.

Mock, M., and A. Fouet, 2001, Anthrax: Annual Review of Microbiology, v. 55, p. 647-671.

Mogridge, J., K. Cunningham, and R. J. Collier, 2002, Stoichiometry of anthrax toxin complexes: Biochemistry, v. 41, p. 1079-1082.

Mongoh, M. N., N. W. Dyer, C. L. Stoltenow, and M. L. Khaitsa, 2007, Characterization of an outbreak of anthrax in animals in North Dakota: The Bovine Practitioner, p. 101-109.

Mongoh, M. N., N. W. Dyer, C. L. Stoltenow, and M. L. Khaitsa, 2008, Risk factors associated with anthrax outbreak in animals in North Dakota, 2005: a retrospective case-control study: Public Health Rep, v. 123, p. 352-359.

Munang'andu, H. M., F. Banda, V. M. Siamudaala, M. Munyeme, C. J. Kasanga, and B. Hamududu, 2012, The effect of seasonal variation on anthrax epidemiology in the upper Zambezi floodplain of western Zambia: J Vet Sci, v. 13, p. 293-298.

Munkhjargal, M., G. Yadamsuren, J. Yamkhin, and L. Menzel, 2020, Ground surface temperature variability and permafrost distribution over mountainous terrain in northern Mongolia: Arctic, Antarctic, and Alpine Research, v. 52, p. 13-26.

Muturi, M., J. Gachohi, A. Mwatondo, I. Lekolool, F. Gakuya, A. Bett, E. Osoro, A. Bitek, S. M. Thumbi, P. Munyua, H. Oyas, O. N. Njagi, B. Bett, and M. K. Njenga, 2018, Recurrent Anthrax Outbreaks in Humans, Livestock, and Wildlife in the Same Locality, Kenya, 2014-2017: Am J Trop Med Hyg, v. 99, p. 833-839.

Nakai, K., and P. Horton, 1999, PSORT: a program for detecting sorting signals in proteins and predicting their subcellular localization: Trends Biochem Sci, v. 24, p. 34-36.

National Statistics Office of Mongolia, Huvsgul Statistics Office.

National Statistics Office of Mongolia, Total number of livestock by 2020.

Odontsetseg, N., T. Sh, Z. Adiyasuren, D. Uuganbayar, and A. S. Mweene, 2007, Anthrax in animals and humans in Mongolia: Rev Sci Tech, v. 26, p. 701-710.

Ohnishi, N., F. Maruyama, H. Ogawa, H. Kachi, S. Yamada, D. Fujikura, I. Nakagawa, M. B. Hang'ombe, Y. Thomas, A. S. Mweene, and H. Higashi, 2014, Genome Sequence of a Bacillus anthracis Outbreak Strain from Zambia, 2011: Genome Announc, v. 2.

Okutani, A., H. Tungalag, B. Boldbaatar, A. Yamada, D. Tserennorov, I. Otgonchimeg, A. Erdenebat, D. Otgonbaatar, and S. Inoue, 2011, Molecular epidemiological study of Bacillus anthracis isolated in Mongolia by multiple-locus variable-number tandem-repeat analysis for 8 loci (MLVA-8): Jpn J Infect Dis, v. 64, p. 345-348.

1553 Pannucci, J., R. T. Okinaka, E. Williams, R. Sabin, L. O. Ticknor, and C. R. Kuske, 2002,
1554 DNA sequence conservation between the Bacillus anthracis pXO2 plasmid and
1555 genomic sequence from closely related bacteria: BMC Genomics, v. 3, p. 34.

1556 Phaswana, P. H., O. C. Ndumnego, S. M. Koehler, W. Beyer, J. E. Crafford, and H. van
1557 Heerden, 2017, Use of the mice passive protection test to evaluate the humoral response
1558 in goats vaccinated with Sterne 34F2 live spore vaccine: Vet Res, v. 48, p. 46.

1559 Pizza, M., V. Scarlato, V. Masignani, M. M. Giuliani, B. Aricò, M. Comanducci, G. T.
1560 Jennings, L. Baldi, E. Bartolini, B. Capecchi, C. L. Galeotti, E. Luzzi, R. Manetti, E.
1561 Marchetti, M. Mora, S. Nuti, G. Ratti, L. Santini, S. Savino, M. Scarselli, E. Storni, P.
1562 Zuo, M. Broeker, E. Hundt, B. Knapp, E. Blair, T. Mason, H. Tettelin, D. W. Hood, A.
1563 C. Jeffries, N. J. Saunders, D. M. Granoff, J. C. Venter, E. R. Moxon, G. Grandi, and
1564 R. Rappuoli, 2000, Identification of vaccine candidates against serogroup B
1565 meningococcus by whole-genome sequencing: Science, v. 287, p. 1816-1820.

1566 Price, E. P., M. L. Seymour, D. S. Sarovich, J. Latham, S. R. Wolken, J. Mason, G. Vincent,
1567 K. P. Drees, S. M. Beckstrom-Sternberg, A. M. Phillippy, S. Koren, R. T. Okinaka, W.
1568 K. Chung, J. M. Schupp, D. M. Wagner, R. Vipond, J. T. Foster, N. H. Bergman, J.
1569 Burans, T. Pearson, T. Brooks, and P. Keim, 2012, Molecular epidemiologic
1570 investigation of an anthrax outbreak among heroin users, Europe: Emerg Infect Dis, v.
1571 18, p. 1307-1313.

1572 Ramisse, V., G. Patra, H. Garrigue, J. L. Guesdon, and M. Mock, 1996, Identification and
1573 characterization of Bacillus anthracis by multiplex PCR analysis of sequences on
1574 plasmids pXO1 and pXO2 and chromosomal DNA: FEMS Microbiol Lett, v. 145, p.
1575 9-16.

1576 Reuveny, S., M. D. White, Y. Y. Adar, Y. Kafri, Z. Altboum, Y. Gozes, D. Kobiler, A.
1577 Shafferman, and B. Velan, 2001, Search for correlates of protective immunity conferred
1578 by anthrax vaccine: Infect Immun, v. 69, p. 2888-2893.

1579 Schlingman, A. S., H. B. Devlin, G. G. Wright, R. J. Maine, and M. C. Manning, 1956,
1580 Immunizing activity of alum-precipitated protective antigen of Bacillus anthracis in
1581 cattle, sheep, and swine: Am J Vet Res, v. 17, p. 256-261.

Sergeev, N., M. Distler, M. Vargas, V. Chizhikov, K. E. Herold, and A. Rasooly, 2006, Microarray analysis of Bacillus cereus group virulence factors: J Microbiol Methods, v. 65, p. 488-502.

Shagdar, E., 2002, The Mongolian livestock sector: Vital for the economy and people, but vulnerable to natural phenomena: Erina Report 08/2002, v. 47, p. 4-26.

Sharkhuu, A., N. Sharkhuu, B. Etzelmüller, E. S. F. Heggem, F. E. Nelson, N. I. Shiklomanov, C. E. Goulden, and J. Brown, 2007, Permafrost monitoring in the Hovsgol mountain region, Mongolia: Journal of Geophysical Research: Earth Surface, v. 112.

Sharkhuu, N., and A. Sharkhuu, 2012, Effects of Climate Warming and Vegetation Cover on Permafrost of Mongolia, *in* M. J. A. Werger, and M. A. van Staalduinen, eds., Eurasian Steppes. Ecological Problems and Livelihoods in a Changing World: Dordrecht, Springer Netherlands, p. 445-472.

Simbotwe, M., D. Fujikura, M. Ohnuma, R. Omori, Y. Furuta, G. M. Muuka, B. M. Hang'ombe, and H. Higashi, 2019, Correction: Development and application of a Bacillus anthracis protective antigen domain-1 in-house ELISA for the detection of anti-protective antigen antibodies in cattle in Zambia, PLoS One, v. 14, p. e0211592.

Sitali, D. C., M. C. Twambo, M. Chisoni, M. J. Bwalya, and M. Munyeme, 2018, Lay perceptions, beliefs and practices linked to the persistence of anthrax outbreaks in cattle in the Western Province of Zambia: Onderstepoort J Vet Res, v. 85, p. 1-8.

Smith, D. B., and K. S. Johnson, 1988, Single-step purification of polypeptides expressed in Escherichia coli as fusions with glutathione S-transferase: Gene, v. 67, p. 31-40.

Stear, M., 2005, OIE Manual of Diagnostic Tests and Vaccines for Terrestrial Animals (Mammals, Birds and Bees) 5th Edn. Volumes 1 & 2. World Organization for Animal Health 2004. ISBN 92 9044 622 6. €140: Parasitology, v. 130, p. 727-727.

Stella, E., L. Mari, J. Gabrieli, C. Barbante, and E. Bertuzzo, 2020, Permafrost dynamics and the risk of anthrax transmission: a modelling study: Sci Rep, v. 10, p. 16460.

Stephens, C., 1998, Bacterial sporulation: a question of commitment?: Curr Biol, v. 8, p. 45-48.

Sutcliffe, I. C., and D. J. Harrington, 2002, Pattern searches for the identification of putative lipoprotein genes in Gram-positive bacterial genomes: Microbiology (Reading), v. 148, p. 2065-2077.

Timofeev, V., I. Bahtejeva, R. Mironova, G. Titareva, I. Lev, D. Christiany, A. Borzilov, A. Bogun, and G. Vergnaud, 2019, Insights from Bacillus anthracis strains isolated from permafrost in the tundra zone of Russia: PLoS One, v. 14, p. e0209140.

Turell, M. J., and G. B. Knudson, 1987, Mechanical transmission of Bacillus anthracis by stable flies (Stomoxys calcitrans) and mosquitoes (Aedes aegypti and Aedes taeniorhynchus): Infect Immun, v. 55, p. 1859-1861.

Turnbull, P. C., 1991, Anthrax vaccines: past, present and future: Vaccine, v. 9, p. 533-539.

Turnbull, P. C., M. G. Broster, J. A. Carman, R. J. Manchee, and J. Melling, 1986, Development of antibodies to protective antigen and lethal factor components of anthrax toxin in humans and guinea pigs and their relevance to protective immunity: Infect Immun, v. 52, p. 356-363.

Turnbull, P. C., M. Doganay, P. M. Lindeque, B. Aygen, and J. McLaughlin, 1992, Serology and anthrax in humans, livestock and Etosha National Park wildlife: Epidemiol Infect, v. 108, p. 299-313.

Van Ness, G. B., 1971, Ecology of anthrax: Science, v. 172, p. 1303-1307.

Vieira, A. R., J. S. Salzer, R. M. Traxler, K. A. Hendricks, M. E. Kadzik, C. K. Marston, C. B. Kolton, R. A. Stoddard, A. R. Hoffmaster, W. A. Bower, and H. T. Walke, 2017, Enhancing Surveillance and Diagnostics in Anthrax-Endemic Countries: Emerg Infect Dis, v. 23, p. 147-153.

Welkos, S. L., and A. M. Friedlander, 1988, Comparative safety and efficacy against Bacillus anthracis of protective antigen and live vaccines in mice: Microb Pathog, v. 5, p. 127-139.

WHO, 2008, Anthrax in humans and animals, World Health Organization.

Yuill, R. S., 1971, The Standard Deviational Ellipse; An Updated Tool for Spatial Description: Geografiska Annaler: Series B, Human Geography, v. 53, p. 28-39.

Ågren, J., M. Finn, B. Bengtsson, and B. Segerman, 2014, Microevolution during an Anthrax outbreak leading to clonal heterogeneity and penicillin resistance: PLoS One, v. 9, p. e89112.